E-Article

# Evolution of Reproduction Periods in Seasonal Environments

**Zepeng Sun,[1,2,3,*] Kalle Parvinen,[4,2] Mikko Heino,[2,5,6,7] Johan A. J. Metz,[2,8,9] André M. de Roos,[1,10] and Ulf Dieckmann[2,11]**

1. Institute for Biodiversity and Ecosystem Dynamics, University of Amsterdam, Amsterdam, The Netherlands; 2. Evolution and Ecology Program, International Institute for Applied Systems Analysis, Laxenburg A-2361, Austria; 3. W. K. Kellogg Biological Station, Michigan State University, Hickory Corners, Michigan 49060; 4. Department of Mathematics and Statistics, University of Turku, Turku FI-20014, Finland; 5. Department of Biological Sciences, University of Bergen, Bergen, Norway; 6. Institute of Marine Research, Bergen, Norway; 7. Institute of Oceanography, National Taiwan University, Taipei, Taiwan; 8. Institute of Biology and Mathematical Institute, Leiden University, The Netherlands; 9. Netherlands Centre for Biodiversity, Naturalis, Leiden, The Netherlands; 10. Santa Fe Institute, Santa Fe, New Mexico 87501; 11. Department of Evolutionary Studies of Biosystems, Graduate University for Advanced Studies (Sokendai), Hayama, Kanagawa 240-0193, Japan

*Submitted November 19, 2018; Accepted November 18, 2019; Electronically published August 11, 2020*

abstract: Many species are subject to seasonal cycles in resource availability, affecting the timing of their reproduction. Using a stage-structured consumer-resource model in which juvenile development and maturation are resource dependent, we study how a species' reproductive schedule evolves, dependent on the seasonality of its resource. We find three qualitatively different reproduction modes. First, continuous income breeding (with adults reproducing throughout the year) evolves in the absence of significant seasonality. Second, seasonal income breeding (with adults reproducing unless they are starving) evolves when resource availability is sufficiently seasonal and juveniles are more efficient resource foragers. Third, seasonal capital breeding (with adults reproducing partly through the use of energy reserves) evolves when resource availability is sufficiently seasonal and adults are more efficient resource foragers. Such capital breeders start reproduction already while their offspring are still experiencing starvation. Changes in seasonality lead to continuous transitions between continuous and seasonal income breeding, but the change between income and capital breeding involves a hysteresis pattern, such that a population's evolutionarily stable reproduction pattern depends on its initial one. Taken together, our findings show how adaptation to seasonal environments can result in a rich array of outcomes, exhibiting seasonal or continuous reproduction with or without energy reserves.

*Keywords:* consumer-resource interactions, eco-evolutionary dynamics, adaptive dynamics, quantitative genetics, seasonal reproduction, changing environments.

* Corresponding author; email: zepengsun@gmail.com.

**ORCIDs:** Sun, https://orcid.org/0000-0002-9846-4174; Parvinen, https://orcid.org/0000-0001-9125-6041; Heino, https://orcid.org/0000-0003-2928-3940; Metz, https://orcid.org/0000-0001-8501-0512; de Roos, https://orcid.org/0000-0002-6944-2048; Dieckmann, https://orcid.org/0000-0001-7089-0393.

Am. Nat. 2020. Vol. 196, pp. E88–E109. © 2020 by The University of Chicago. 0003-0147/2020/19604-58880$15.00. All rights reserved. This work is licensed under a Creative Commons Attribution-NonCommercial 4.0 International License (CC BY-NC 4.0), which permits non-commercial reuse of the work with attribution. For commercial use, contact journalpermissions@press.uchicago.edu. DOI: 10.1086/708274

## Introduction

Climate change can have strong influences on biodiversity, ecosystems, and ecosystem services (e.g., Parmesan et al. 1999; Richardson and Schoeman 2004; Hoegh-Guldberg and Bruno 2010; Grimm et al. 2013). Shifts in phenology—that is, the timing of life-cycle events—are among the best-known biological responses to climate change (Thackeray et al. 2016), empirically documented in plants (Chuine et al. 2004; Cleland et al. 2006; Piao et al. 2019), migratory birds (Norris et al. 2004; Lamires et al. 2018), insects (Roy and Sparks 2000; Altermatt 2010), and marine systems (Edwards and Richardson 2004; Henson et al. 2018).

Of all the timings in species' life cycles affected by climate change, the timing of reproduction (or breeding) is arguably the most important one, since adjusting reproductive timing to climate condition is essential for reproductive success (Lustenhouwer et al. 2018). The negative impacts of climate change on reproductive success mainly result from a seasonal mismatch between a population's food requirements and the corresponding food availabilities (van Asch et al. 2013). In marine biology, this is well known as the so-called match-mismatch hypothesis, stating that if the timing of offspring production matches the seasonal peak in food availability (e.g., the spring bloom of phytoplankton), effective recruitment will be high, whereas a mismatch between offspring food requirement and food availability will lead to low effective recruitment (Cushing 1969). In the context of climate change, this idea has typically been discussed using the terms "phenological mismatch" and "trophic asynchrony" (Stenseth and Mysterud 2002; Renner and Zohner 2018). Typical examples include breeding in birds, where climate change could greatly affect reproductive success when birds have been knocked out of sync with their chicks' food supply (Visser et al.

1998; Knudsen et al. 2011). However, phenological mismatch does not necessarily involve trophic interactions. In plants, for example, leaf unfolding responds to direct temperature effects (Renner and Zohner 2018), which can lead to a mismatch involving a nonconsumptive interspecific interaction. Heberling et al. (2019) reported a mismatch between the overstory tree leaf out and understory wildflower phenology due to increased spring temperature, which may lead to the decline of these wildflower species.

Animals and plants use environmental cues to time their life-cycle events. While these cues can be fixed (photoperiod; e.g., Kjesbu et al. 2010), most of them are naturally variable (e.g., temperature, rainfall), and phenology is often phenotypically plastic (Nussey et al. 2007; Nicotra et al. 2010; Knudsen et al. 2011). However, phenological reaction norms that have evolved under past climatic fluctuations may prove maladaptive under rapidly changing climate. Climate change is therefore expected to be a driver of evolutionary change in wild animals and plants (Bradshaw and Holzapfel 2006), although teasing apart phenotypically plastic and genetic responses is challenging (Merilä and Hendry 2014).

The evolution of reproductive strategies in seasonal environments has also attracted theoretical interest. Early studies focused on environmental variability in general (e.g., King and Roughgarden 1982; Iwasa and Levin 1995; Yamamura et al. 2007), while more recent ones focused on climate change in particular (e.g., Jonzén et al. 2007; Johansson et al. 2013; Kristensen et al. 2015; Lindh et al. 2016). The models studied until now typically involve a number of simplifications that restrict the questions they can address and have often been geared to situations motivated by the phenologies of annual plants or seasonally breeding birds: (1) organisms can decide when to start reproducing but have no further flexibility to adjust the time course of their reproductive activity; (2) feedback between organisms and their environment is one-directional: organisms are affected by the environment, but there is no feedback from the organisms back to the environment, such as exhaustion of resources; and (3) adult and juvenile individuals do not compete for the same resources. Here we relax these three simplifying assumptions simultaneously in order to understand how phenology of reproduction—which we characterize by its starting time and duration—evolves in organisms in which adults and juveniles share the same habitat and consume the same renewable resource. This is relevant for understanding phenology in organisms with overlapping generations and no parental care, as is the case for perennial plants and for many invertebrates and aquatic animals—types of organisms that earlier research has largely ignored.

Methodologically, our study is motivated by advances in modeling consumer-resource systems with resource-dependent juvenile development and sexual maturation (e.g., de Roos et al. 2007; Guill 2009; Sun and de Roos 2017) rather than the classic Lotka-Volterra-type models that consider only the resource-dependent reproduction of adults. A key feature of these consumer-resource models is whether a so-called energetic asymmetry between the two consumer stages is present, reflecting their relative competitiveness (de Roos et al. 2013; Persson and de Roos 2013). Such asymmetry may arise, for example, because of different energy budgets for the juvenile and adult stages, in particular, when juveniles and adults are feeding on separate resources with different productivities or when they are feeding on a shared resource with different ingestion rates. Because of this asymmetry, the consumer population might be primarily regulated by either the development of juveniles or the reproduction of adults (de Roos et al. 2007).

In this article, we extend the stage-structured consumer-resource model by Sun and de Roos (2017) to investigate how reproductive strategies can evolve in a population that is dynamically coupled to its resource and living in a seasonally varying environment. Using analyses based on the theories of adaptive dynamics (Dieckmann and Law 1996; Metz et al. 1996; Geritz et al. 1998) and quantitative genetics (Lande 1979, 1982; Iwasa et al. 1991), we investigate the evolutionary outcomes as a result of different resource-growth patterns and different energetics of the consumer population. Our model predicts the emergence of two qualitatively different types of reproduction modes that correspond to the prevailing use (Stephens et al. 2009) of the terms "capital breeding" (in which reproduction is financed at least partly by reproductive energy reserves) and "income breeding" (in which reproduction is financed by concurrent intake only). Furthermore, our model predicts how income breeding may be either continuous or seasonal. Taken together, our model predicts three qualitatively different reproduction modes (fig. 1): (A) continuous income breeding, with adults reproducing throughout the year; (B) seasonal income breeding, with adults reproducing unless they are starving; and (C) seasonal capital breeding, with adults reproducing partly through the use of energy reserves. The last mode may or may not involve the periodic starvation of adults (C1 and C2).

## Model Description

### *Population Dynamics*

We base the population dynamics of our model on the consumer-resource biomass model introduced by de Roos et al. (2008), which has been derived as a simplification of a fully size-structured population model. The model accounts for one shared resource with density $R$ and a stage-structured consumer population.

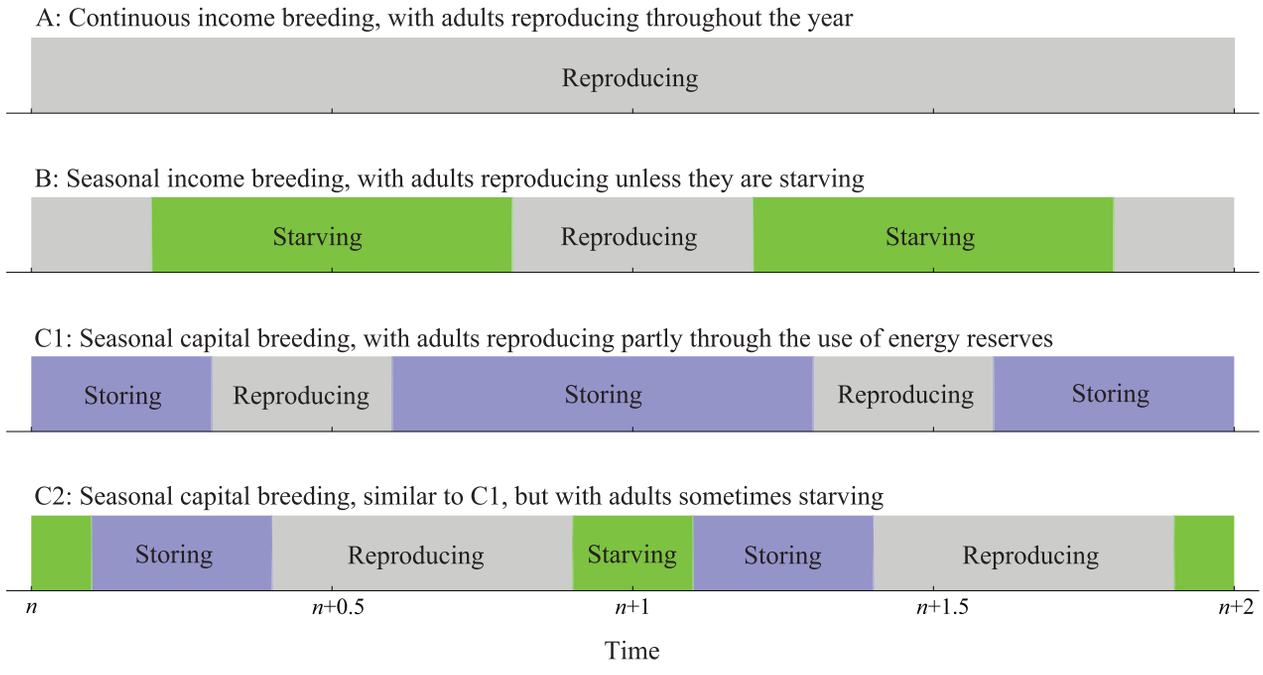


**Figure 1:** Schematic illustration of the different reproduction modes predicted by our analyses. In all panels, gray shading marks the reproduction periods of adults, green shading marks the periods during which adults starve, and blue shading marks the periods during which adults are storing energy for reproduction.

To reduce the number of parameters without loss of generality, we scale time so as to fix the duration of one seasonal cycle (e.g., 1 year) to 1. Figure 2 illustrates the processes taking place at different times within such cycle, as we explain in detail below. The resource follows a semichemostat growth dynamics with a periodic growth rate

$$G(R) = \left[1 + \omega \frac{f(t) - f(0)}{f(0.5) - f(0)}\right](R_{\max} - R), \qquad (1a)$$

where

$$f(t) = \exp\left(-\frac{1}{2}[\mathrm{mod}(t, 1) - 0.5]^2/\alpha^2\right) \qquad (1b)$$

is a periodic function with period 1 and $R_{\max}$ is the maximum density the resource can reach in the absence of consumers. The resource growth rate is modeled by combining a baseline value with a unimodal function of time: the parameter $\omega$ determines the oscillation amplitude of the resource growth rate, and $\alpha$ is the standard deviation determining the width of the resource growth rate peak. Because, for a fixed oscillation amplitude and peak width, a time shift of the position of the resource growth rate peak merely leads to a corresponding time shift of the population dynamics, we fix the peak of the resource growth rate at $t = 0.5$ without loss of generality.

Following de Roos et al. (2008), we assume that the consumer individuals are distinguished by their body size, denoted by $s$. All consumer individuals are born with the same body size $s_b$ and mature at body size $s_m$. The consumer population is thus divided into two stages: juvenile stage and adult stage. The total biomasses of juveniles and adults are denoted by $J$ and $A$, respectively. We further assume that adults invest all their net energy gain (i.e., the difference between resource assimilation and maintenance costs) in reproduction or storage and hence do not grow in structural body mass. Moreover, resource ingestion and maintenance costs are both assumed to be proportional to body mass.

The resource is consumed by juveniles and adults following a linear functional response:

$$\frac{dR}{dt} = G(R) - a(J + \theta A)R. \qquad (2)$$

Here, $a$ is the intake rate per unit body mass of juveniles, and $\theta$ is the intake rate of adults relative to juveniles, which reflects the competitive ability of adults in terms of resource intake compared with juveniles. Accordingly, the intake rate per unit body mass of adults is $\theta a$.

Ingested resource biomass is converted into consumer biomass with conversion efficiencies $\sigma_j$ and $\sigma_a$ for juveniles and adults, respectively. The maintenance requirement

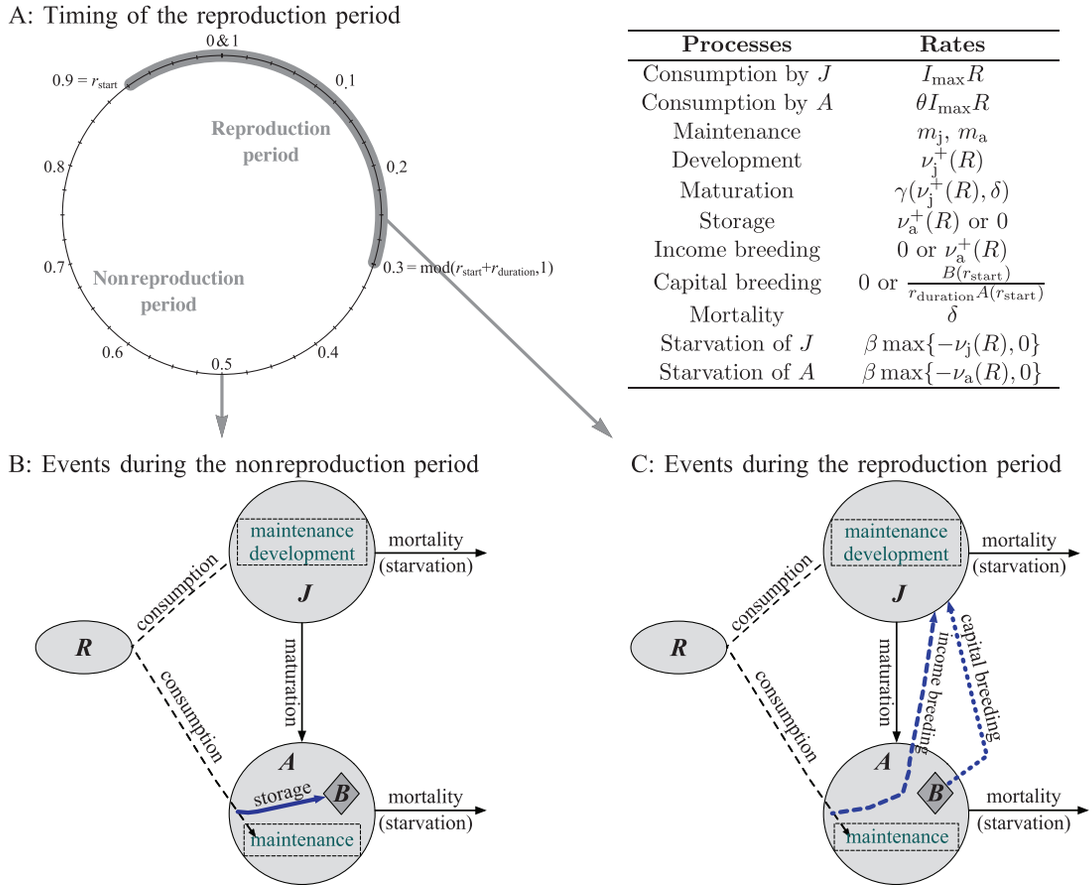


| Processes | Rates |
|---|---|
| Consumption by $J$ | $I_{\max}R$ |
| Consumption by $A$ | $\theta I_{\max}R$ |
| Maintenance | $m_{\mathrm{j}}$, $m_{\mathrm{a}}$ |
| Development | $\nu_{\mathrm{j}}^{+}(R)$ |
| Maturation | $\gamma(\nu_{\mathrm{j}}^{+}(R),\delta)$ |
| Storage | $\nu_{\mathrm{a}}^{+}(R)$ or 0 |
| Income breeding | 0 or $\nu_{\mathrm{a}}^{+}(R)$ |
| Capital breeding | 0 or $\frac{B(r_{\mathrm{start}})}{r_{\mathrm{duration}}A(r_{\mathrm{start}})}$ |
| Mortality | $\delta$ |
| Starvation of $J$ | $\beta\max\{-\nu_{\mathrm{j}}(R),0\}$ |
| Starvation of $A$ | $\beta\max\{-\nu_{\mathrm{a}}(R),0\}$ |

**Figure 2:** Life-history events during the nonreproduction period (*B*) and reproduction period (*C*). *A* illustrates how the timing of the reproduction period (thick gray line) and nonreproduction period (thin black line) depends on the reproductive strategy ($r_{\mathrm{start}}$, $r_{\mathrm{duration}}$). We illustrate the values $(r_{\mathrm{start}}, r_{\mathrm{duration}}) = (0.9, 0.4)$. The considered life-cycle processes are listed together with their rates. In *B* and *C*, the blue arrows distinguish between the processes of energy storage (solid blue line), income breeding (dashed blue line), and capital breeding (dotted blue line) of adults (the same line styles are also used in figs. 3 and 4).

per unit body mass for juveniles and adults is denoted by $m_{\mathrm{j}}$ and $m_{\mathrm{a}}$, respectively. The net biomass production per unit body mass of juveniles and that of adults, denoted by $\nu_{\mathrm{j}}(R)$ and $\nu_{\mathrm{a}}(R)$, respectively, equal the balance between their requirements for assimilation and maintenance,

$$\nu_{\mathrm{j}}(R) = \sigma_{\mathrm{j}}aR - m_{\mathrm{j}}, \tag{3a}$$

$$\nu_{\mathrm{a}}(R) = \sigma_{\mathrm{a}}\theta aR - m_{\mathrm{a}}. \tag{3b}$$

At low densities of the resource, the ingestion may not be sufficient to cover an individual's maintenance, in which case the individuals are experiencing a starvation mortality rate proportional to the energy deficit. The per capita starvation mortality rate equals $\beta\max\{-\nu_{\mathrm{j}}(R), 0\}$ and $\beta\max\{-\nu_{\mathrm{a}}(R), 0\}$ for the juvenile and adult stages, respectively. Here, $\beta$ is the proportionality constant relating the starvation rate and mortality rate of the consumer. The per capita background mortality rate of consumers, $\delta$, is assumed to be equal for the two stages. The total per capita mortality rate of the individuals is the sum of the background and the starvation mortality rates,

$$d_{\mathrm{j}}(R) = \delta + \beta\max\{-\nu_{\mathrm{j}}(R), 0\}, \tag{4a}$$

$$d_{\mathrm{a}}(R) = \delta + \beta\max\{-\nu_{\mathrm{a}}(R), 0\}. \tag{4b}$$

Following de Roos et al. (2008) and Sun and de Roos (2017), we assume that the development and maturation of juveniles as well as the reproduction of adults halt when the individuals are starving. We introduce $\nu_{\mathrm{j}}^{+}(R)$ and $\nu_{\mathrm{a}}^{+}(R)$ to restrict the net biomass production per unit body mass of juveniles and adults to nonnegative values,

$$\nu_{\mathrm{j}}^{+}(R) = \max\{\nu_{\mathrm{j}}(R), 0\}, \tag{5a}$$

$$\nu_{\mathrm{a}}^{+}(R) = \max\{\nu_{\mathrm{a}}(R), 0\}. \tag{5b}$$

Throughout the seasonal cycle, juvenile biomass increases through growth in body size at the rate $\nu_j^+(R)$, decreases because of mortality at the rate $d_j(R)$, and decreases because of maturation at the mass-specific rate $\gamma(\nu_j^+(R), \delta)$ (de Roos et al. 2008), with

$$\gamma(\nu, \delta) = \frac{\nu - \delta}{1 - z^{1-\delta/\nu}}. \tag{6}$$

Here, $z = s_b/s_m < 1$ is the ratio of individual body size at birth and as an adult. This maturation rate takes into account that juveniles can grow in body size only when they have positive net biomass production (i.e., when $\nu_j(R) > 0$) and that a high mortality $\delta$ decreases the likelihood that juveniles survive until maturation. Note that the function $\gamma(\nu, \delta)$ is continuous and smooth for positive $\nu$ and $\delta$ (also around $\nu \approx \delta$) and that $\gamma(\nu, \delta)$ tends to zero when $\nu \to 0^+$ (from the positive side; see also fig. A1). Adult biomass increases because of maturation from the juvenile stage and decreases because of mortality at the rate $d_a(R)$.

Unlike continuous-time consumer-resource biomass models (e.g., de Roos et al. 2007, 2008), we consider the reproduction of adults to be seasonal. We assume that the seasonal cycle is divided into two parts (fig. 2*A*): a nonreproduction period (fig. 2*B*) and a reproduction period (fig. 2*C*). Adults are assumed to consume the resource and die of background mortality—and possibly of starvation mortality—continuously throughout the seasonal cycle and reproduce only during reproduction periods. During nonreproduction periods, adults convert all their net biomass production into energy storage in their bodies, the total amount of which in the entire population is denoted by $B$ (fig. 2*B*). This storage decays with the adult mortality rate, since when an adult individual dies its energy reserves are lost as well. Furthermore, since it is empirically not yet very clear whether organisms actually need to pay biologically significant maintenance costs for their reproductive energy storage (Kooijman 2000), in this study we assume that this cost is so small as to be negligible.

Adults can differ in their timing of reproduction, determined by their reproductive strategy. The starting time of the reproduction period is determined by the strategy component $r_{start}$ and the duration by $r_{duration}$. For example, individuals with strategy $(r_{start}, r_{duration}) = (0.9, 0.4)$, as illustrated in figure 2*A*, reproduce during $0.9 \le t \le 0.9 + 0.4 = 1.3$, during $1.9 \le t \le 2.3$, during $2.9 \le t \le 3.3$, and so on. Individuals with $r_{duration} = 1$ reproduce all the time.

During reproduction periods (fig. 2*C*), adults convert all their net biomass production into offspring that enter the juvenile stage (income breeding). Furthermore, the energy storage is released by adults as offspring (capital breeding). We assume that each adult releases its energy storage at a constant speed in such a manner that the energy storage becomes empty precisely at the end of each reproduction period. Short reproduction periods thus correspond to a fast release of the energy storage. The dynamics of the consumer population are given by the following ordinary differential equation system.

1. During nonreproduction periods, that is, when $t \notin [n + r_{start}, n + r_{start} + r_{duration}]$ for some $n$, indicating the integer-valued index of the year,

$$\frac{dJ}{dt} = \nu_j^+(R)J - \gamma(\nu_j^+(R), \delta)J - d_j(R)J, \tag{7a}$$

$$\frac{dA}{dt} = \gamma(\nu_j^+(R), \delta)J - d_a(R)A, \tag{7b}$$

$$\frac{dB}{dt} = \nu_a^+(R)A - d_a(R)B, \; B(n + r_{start} + r_{duration}) = 0. \tag{7c}$$

2. During reproduction periods, that is, when $t \in [n + r_{start}, n + r_{start} + r_{duration}]$ for some $n$,

$$\frac{dJ}{dt} = \nu_j^+(R)J - \gamma(\nu_j^+(R), \delta)J - d_j(R)J + \nu_a^+(R)A + \frac{B_{max}}{r_{duration}}, \tag{8a}$$

$$\frac{dA}{dt} = \gamma(\nu_j^+(R), \delta)J - d_a(R)A, \tag{8b}$$

$$\frac{dB_{max}}{dt} = -d_a(R)B_{max}, \; B_{max}(n + r_{start}) = B(n + r_{start}), \tag{8c}$$

$$B(t) = B_{max}(t)\frac{n + r_{start} + r_{duration} - t}{r_{duration}}. \tag{8d}$$

Here, as shown in figure 2, $B$ quantifies the reproductive energy reserves of adults, which accrue only during the nonreproductive periods and decay during the reproduction periods. Furthermore, in order to specify the reproductive behavior described above, we have introduced the dynamical variable $B_{max}$ to represent the stored energy reserves present at time $t = n + r_{start}$ discounted with the adult mortality that occurred since the start of the reproduction period. This modeling of the reproduction based on stored energy reserves using $B_{max}$ ensures that adult individuals empty their energy reserves at a constant rate and reach zero energy reserves at the end of the reproduction period, while accounting for adult mortality.

In this article, we assume for the sake of simplicity that the maintenance costs and conversion efficiencies of juveniles and adults are the same. As it turns out, the energetic asymmetry caused by different maintenance costs or conversion efficiencies of juveniles and adults has a similar qualitative effect on model predictions as the

intake ratio, which we are studying in detail. Furthermore, we assume that the background mortality rate in the juvenile and adult stages are the same, since increasing the adult mortality rate has an analogous effect as decreasing the adult intake rate, while increasing the juvenile mortality rate has only some quantitative effects on model predictions. All parameters and functions of the model are summarized in table 1.

### *Evolutionary Dynamics*

We use the theories of adaptive dynamics (Dieckmann and Law 1996; Metz et al. 1996; Geritz et al. 1998) and quantitative genetics (Lande 1979, 1982; Iwasa et al. 1991) to study the evolution of the reproductive strategy of the stage-structured consumer population. We focus on the evolution of the starting time $r_{\text{start}}$ and the duration $r_{\text{duration}}$ of the reproduction periods. We denote by $F((r_{\text{start}}, r_{\text{duration}}), (r'_{\text{start}}, r'_{\text{duration}}))$ the invasion fitness, that is, the long-term exponential growth rate of rare variants with traits $(r'_{\text{start}}, r'_{\text{duration}})$ in the environment established by a resident population with traits $(r_{\text{start}}, r_{\text{duration}})$.

The selection gradient for traits $(r_{\text{start}}, r_{\text{duration}})$, describing the direction and strength of selection, is denoted by $(g_{r_{\text{start}}}(r_{\text{start}}, r_{\text{duration}}), g_{r_{\text{duration}}}(r_{\text{start}}, r_{\text{duration}}))$. Its two components are defined as the derivatives of the invasion fitness with respect to $r'_{\text{start}}$ and $r'_{\text{duration}}$, respectively, and are evaluated for values of the variant traits equal to those of the resident. We derive the invasion fitness as the dominant eigenvalue of the yearly growth matrix of the rare mutant, and furthermore, we use the eigenvalue sensitivity (Caswell 2001) as a numerically efficient method to compute the selection gradient; the mathematical expressions for the invasion fitness and the selection gradient can be found in appendix B.

In adaptive dynamics theory, the evolutionary dynamics resulting from the selection gradient are described by the canonical equation (Dieckmann and Law 1996):

$$\frac{\mathrm{d}}{\mathrm{d}t}\begin{pmatrix} r_{\text{start}} \\ r_{\text{duration}} \end{pmatrix} = \frac{1}{2}\mu\bar{n}(r_{\text{start}}, r_{\text{duration}})\mathbf{M}\begin{pmatrix} g_{r_{\text{start}}}(r_{\text{start}}, r_{\text{duration}}) \\ g_{r_{\text{duration}}}(r_{\text{start}}, r_{\text{duration}}) \end{pmatrix}, \tag{9a}$$

where $\mu$ is the mutation ratio per birth event, $\bar{n}$ is the effective population size (e.g., Metz and de Kovel 2013), and $\mathbf{M}$ is the variance-covariance matrix of the bivariate mutation distribution.

In quantitative genetics theory, the evolutionary dynamics resulting from the selection gradient are described by Lande's equation (Lande 1979, 1982), or, more accurately, by its generalization to frequency-dependent selection (Iwasa et al. 1991):

$$\frac{\mathrm{d}}{\mathrm{d}t}\begin{pmatrix} r_{\text{start}} \\ r_{\text{duration}} \end{pmatrix} = \mathbf{G}\begin{pmatrix} g_{r_{\text{start}}}(r_{\text{start}}, r_{\text{duration}}) \\ g_{r_{\text{duration}}}(r_{\text{start}}, r_{\text{duration}}) \end{pmatrix}, \tag{9b}$$

where $\mathbf{G}$ is the variance-covariance matrix of the distribution of standing additive genetic variation.

The mutation ratio and population size in equation (9a) affect only the speed (but not the trajectories) of evolutionary change and can therefore be ignored when examining the latter. The matrices $\mathbf{M}$ or $\mathbf{G}$ affect the shape of the evolutionary trajectories and thus may affect whether evolution converges to them, but they do not affect the location of the evolutionary endpoints. We therefore use identity matrices $\mathbf{M}$ or $\mathbf{G}$ for illustrating our results, corresponding

**Table 1:** Model parameters with their default values and model functions

| | Value | Definition |
|---|---|---|
| Parameter: | | |
| $\omega$ | Varied | Oscillation amplitude of the resource growth rate |
| $\alpha$ | Varied | Peak width of the resource growth rate |
| $r_{\text{start}}$ | Evolving | Starting time of the consumer reproduction period |
| $r_{\text{duration}}$ | Evolving | Duration of the consumer reproduction period |
| $R_{\max}$ | 2 | Maximum density of the resource |
| $a$ | 10 | Intake rate per unit body mass of juveniles |
| $m_{\text{j}}$, $m_{\text{a}}$ | 1 | Maintenance cost per unit body mass of juveniles and adults |
| $\sigma_{\text{j}}$, $\sigma_{\text{a}}$ | .5 | Conversion efficiency of juveniles and adults |
| $\theta$ | Varied | Mass-specific intake rate of adults relative to juveniles |
| $\delta$ | .1 | Stage-independent consumer background mortality rate |
| $\beta$ | 1 | Proportion of mortality rate related to starvation rate of consumers |
| Function: | | |
| $B_{\max}$ | | Total energy storage at the beginning of the reproduction period |
| $\nu_{\text{j}}(R)$, $\nu_{\text{a}}(R)$ | | Net biomass production per unit body mass of juveniles and adults |
| $d_{\text{j}}(R)$, $d_{\text{a}}(R)$ | | Total per capita mortality rate of juveniles and adults |
| $\gamma(\nu, \delta)$ | | Mass-specific maturation rate of juveniles |

to independent evolution of the start and duration of the reproduction period. Furthermore, we demonstrate as part of our results that the two components of the selection gradient are of different magnitude, which makes the two-dimensional evolutionary dynamics effectively one-dimensional. Thus, our results concerning the shape of evolutionary trajectories and the location and convergence stability of evolutionary end points are all independent of the considered matrices and equally apply to evolutionary dynamics described by adaptive dynamics theory or quantitative genetics theory.

The evolutionary dynamics in equation (9a) are numerically integrated (using Mathematica) for different initial trait values ($r_{\text{start},0}$, $r_{\text{duration},0}$), leading to evolutionary phase portraits in trait space, from which the evolutionary end points are inferred.

## Results

The semi-time-discrete consumer-resource model we study here has been shown always to exhibit stable fixed-point dynamics in the time-discrete component of its dynamics (Sun and de Roos 2017). In this section, we investigate the evolution of the reproductive strategy ($r_{\text{start}}$, $r_{\text{duration}}$), given by the starting time $r_{\text{start}}$ and the duration $r_{\text{duration}}$ of the reproduction period, for different seasonal patterns of the resource growth rate, as determined by its oscillation amplitude $\omega$ and peak width $\alpha$. A key parameter affecting the evolutionary outcome is the adult-juvenile intake ratio $\theta$.

### *Without Adult Starvation, Evolution Results in Either Continuous Income Breeding or Seasonal Capital Breeding*

Our model predicts that without adult starvation, evolution can result in either continuous income breeding (with adults reproducing throughout the seasonal cycle) or seasonal capital breeding (with adults reproducing partly through the use of stored energy reserves). The latter happens, for example, for relatively high values of the adult-juvenile intake ratio $\theta$. The within-season dynamics resulting from such reproductive strategies are illustrated in figure 3. The solid black lines in the top panels show the resource density. Juveniles have a positive starvation rate (red line) when the resource density falls below the corresponding threshold level (dashed lines). In this figure, juveniles do starve (yellow shading), but the resource intake rate of adults relative to juveniles, $\theta$, is so large that adults never starve. The middle panels illustrate the actual reproduction behavior of adults, and the bottom panels show the resulting population densities.

If the resource growth rate oscillates only little throughout the seasonal cycle (left column of fig. 3), the reproduction period (gray shading) stretches across the whole seasonal cycle. Therefore, reproduction consists solely of income breeding (with rate $\nu_{\text{a}}^{+}(R)$), and the rates of storing and storage release are zero. As a consequence, the energy storage remains at zero (bottom panel). Following Stephens et al. (2009), we refer to such a reproductive strategy as continuous income breeding (with no adult starvation; IN).

In case of substantial seasonal variations in the resource growth rate (right column of fig. 3), adults have a distinct reproduction period (gray shading). During the nonreproduction period, adults store their excess energy. During the reproduction period, the total reproduction rate per unit biomass thus consists of storage release, at rate $B(r_{\text{start}})/[r_{\text{duration}}A(r_{\text{start}})]$ (dotted blue line), plus income breeding, at rate $\nu_{\text{a}}^{+}(R)$ (dashed blue line). We refer to such a reproductive strategy as seasonal capital breeding (with no adult starvation; CN) because reproduction is seasonal and at least a part of breeding is based on stored energy. Here, the total energy storage $B$ and the total adult biomass $A$ in the storage-release rate are evaluated at $t = r_{\text{start}}$, since they decay because of mortality at the same rate $d_{\text{a}}(R)$.

### *Starvation of Adults Can Result in Seasonal Income Breeding*

When adults are less efficient in their energy intake, they starve during part of the seasonal cycle. Under these conditions, our model predicts two alternative evolutionary outcomes when the seasonal oscillations in the resource growth rate are substantial.

In one evolutionary outcome, reproduction is strictly based on income and occurs whenever it is energetically possible. Such a reproductive strategy is seasonal because starving adults cannot reproduce. Therefore, we refer to it as seasonal income breeding, which involves adult starvation (IS). This is illustrated in the left column of figure 4, in which the reproduction period (gray shading) corresponds precisely to the nonstarvation period of adults (absence of green shading).

In the other evolutionary outcome, part of the period during which adults have a positive energy balance is used to build up storage to boost reproduction during the next season. Capital breeding can thus evolve also under adult starvation (CS). The right column of figure 4 illustrates such a reproductive strategy, for which the reproduction period (gray shading) does not extend to the whole nonstarvation period of adults (absence of green shading). Similar to the right column of figure 3, the total reproduction rate consists of the storage-release rate (dotted

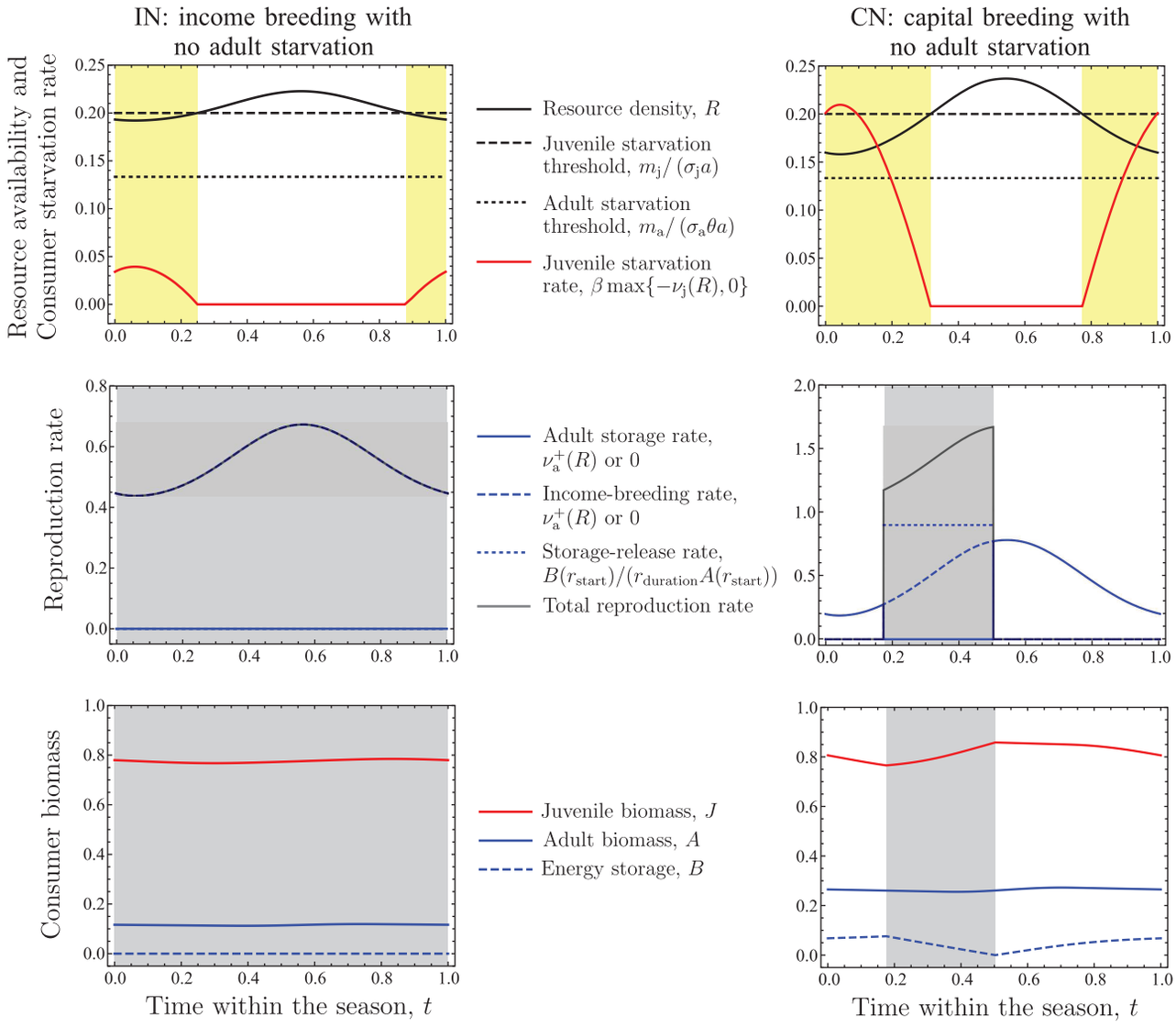


**Figure 3:** Without adult starvation, evolution results in either continuous income breeding or seasonal capital breeding. The top panels show the within-season dynamics of the resource density and the starvation rate of juveniles; the yellow area shows the periods during which juveniles are starving, and the two horizontal lines show the thresholds below which juveniles and adults are starving. The middle panels show the reproduction period (gray area) and the reproduction rates by adults, including the per capita storage-release rate $B(r_{start})/[r_{duration}A(r_{start})]$ and the income-breeding rate $\nu_a^+(R)$. The bottom panels show the reproduction period and the consumer biomass densities. In the left column, $\omega = 0.2$ and the reproductive strategy is $(r_{start}, r_{duration}) = (0, 1)$. In the right column, $\omega = 0.7$ and the reproductive strategy is $(r_{start}, r_{duration}) = (0.18, 0.33)$. In all panels, $\theta = 1.5$, $\alpha = 0.2$, and all other parameters have the default values shown in table 1.

blue line) and the income-breeding rate (dashed blue line).

### *Capital Breeding and Income Breeding May Alternatively Evolve under the Same Conditions*

The evolutionary outcomes for the reproductive strategies in our model are globally attracting for a majority range of parameter values, so that the evolutionary end point does not depend on a population's initial reproductive strategy. Under some conditions, however, capital breeding and income breeding can alternatively evolve, depending on the initial reproductive strategy. We illustrate such bistability using evolutionary phase portraits showing the trajectories resulting from equation (9a). Since time is periodic, it is natural to use polar coordinates, with the angle representing the starting time of the reproduction period and with the distance to the boundary circle

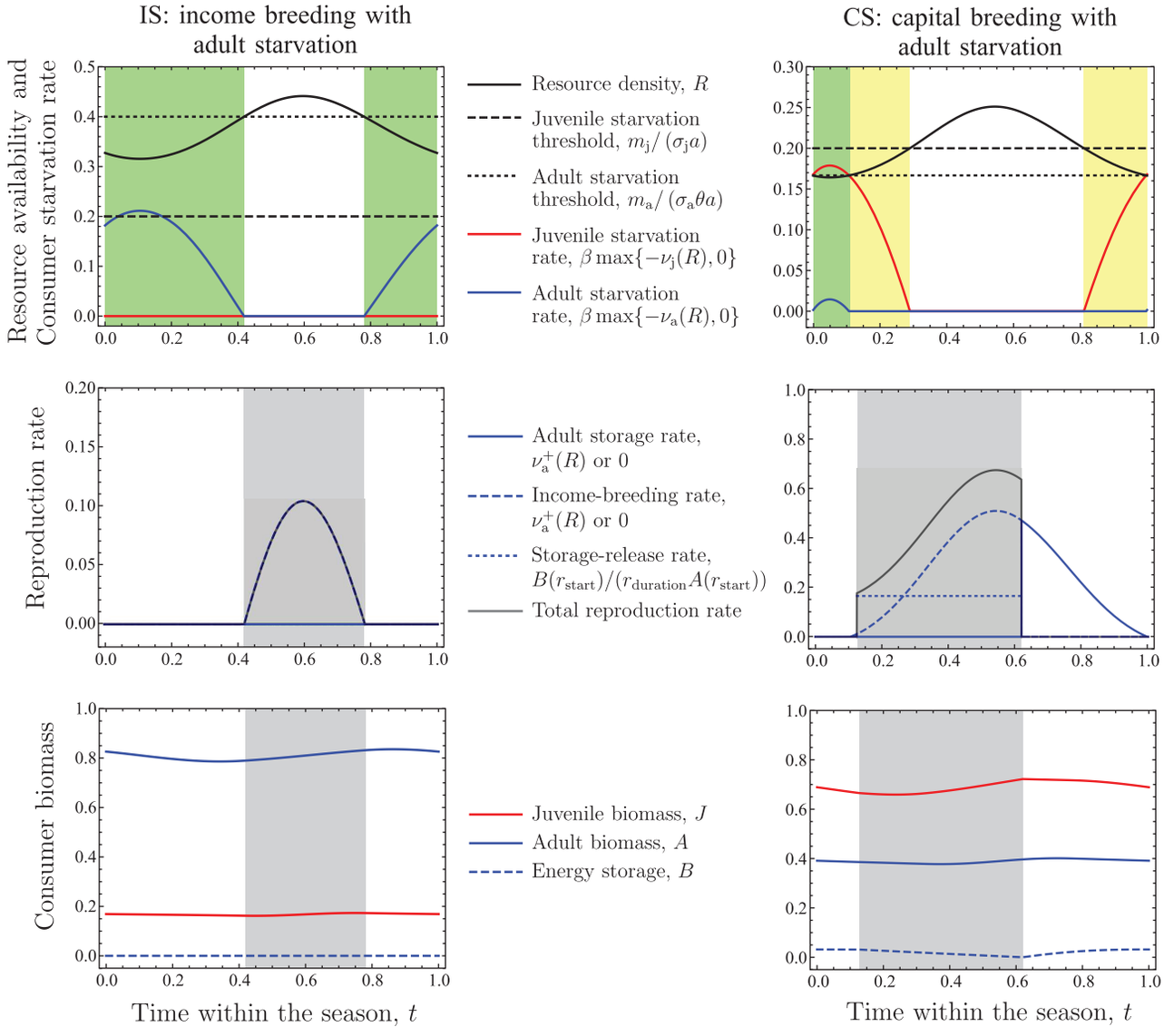


**Figure 4:** Starvation of adults can result in seasonal income breeding. In addition to the elements already shown in figure 3 and explained there, the adult starvation period is indicated by the green areas, and the adult starvation rate is indicated in the top panels. In the left column, $\theta = 0.5$ and the reproduction period is identical to the nonstarvation period of adults, characterized by the reproductive strategy $(r_{\text{start}}, r_{\text{duration}}) = (0.42, 0.36)$. In the right column, $\theta = 1.2$ and the reproductive strategy is $(r_{\text{start}}, r_{\text{duration}}) = (0.13, 0.49)$. In all panels, $\omega = 0.7$, $\alpha = 0.2$, and all other parameters have the default values shown in table 1.

representing the duration of the reproduction period (fig. 5). At the central point of these polar diagrams, the duration of the reproduction period equals 1, which, in the absence of adult starvation, indicates that adults reproduce continuously, so that the starting time is irrelevant. The left column of figure 5 shows phase portraits with no adult starvation, while the right column shows phase portraits with adult starvation.

Figure 5*A*–5*D* show the evolutionary phase portraits for globally attracting reproductive strategies corresponding to the model dynamics shown in figures 3 and 4. Note that the small areas of shading in the centers of figures 5*B* and 5*D* are in different colors, indicating that in figure 5*B* seasonal income breeding is attracting (as in fig. 4*B*), whereas in figure 5*D* it is not.

Figure 5*E* illustrates bistability with no adult starvation (BN). If the initial reproductive strategy at the beginning of an evolutionary trajectory is close to the central point—that is, the orange circle corresponding to continuous income breeding (IN)—then the trajectory

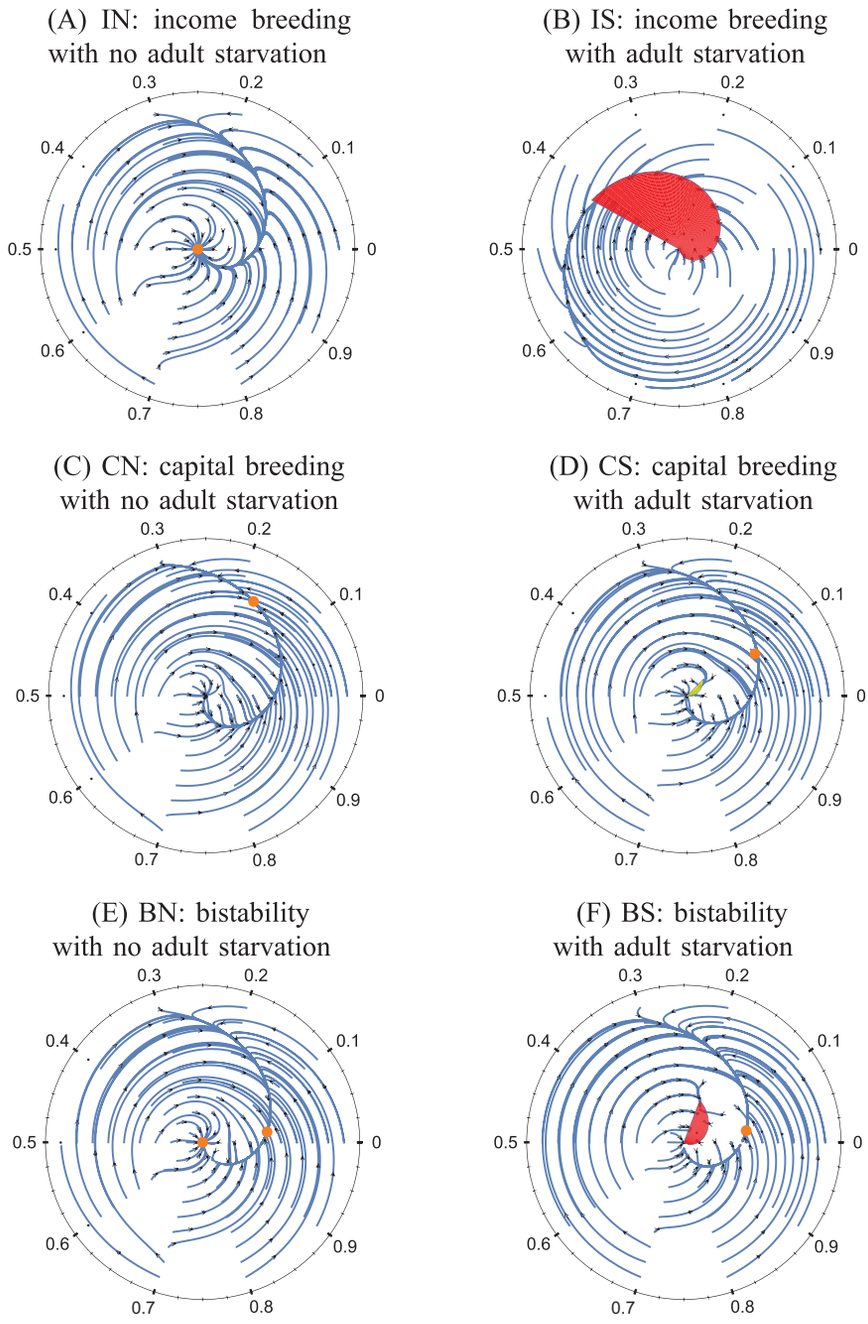


**Figure 5:** Capital breeding and income breeding may alternatively evolve under the same conditions. *A*–*D* show phase portraits with globally attractive reproductive strategies, while *E* and *F* show phase portraits with evolutionary bistability, illustrating how the initial reproductive strategy can affect the evolutionary outcome. *E*, Bistability between continuous income breeding (orange circle at center) and seasonal capital breeding (orange circle outside of center) without adult starvation (BN). *F*, Bistability between seasonal income breeding (red area) and seasonal capital breeding (orange circle) with adult starvation (BS). Arrows indicate the direction of evolution. The evolving traits are depicted in polar coordinates, with the angle indicating the starting time of the reproduction period and the distance to the boundary circle indicating the duration of the reproduction period. The red and yellow areas in *B*, *D*, and *F* comprise the reproductive strategies for which adults reproduce when they can, so that the nonstarvation period of adults is completely contained within their period of attempted reproduction. The red areas are evolutionarily attracting, while the small yellow area in *D* is evolutionarily repelling. In *A*, $\theta = 1.5$ and $\omega = 0.2$; in *B*, $\theta = 0.5$ and $\omega = 0.7$; in *C*, $\theta = 1.5$ and $\omega = 0.7$; in *D*, $\theta = 1.2$ and $\omega = 0.7$; in *E*, $\theta = 1.3$ and $\omega = 0.4$; and in *F*, $\theta = 1.16$ and $\omega = 0.9$. In all panels, $\alpha = 0.2$, and all other parameters have the default values shown in table 1.

will converge to that point. Analogously, if the initial reproductive strategy is close to the other evolutionary endpoint—that is, the other orange circle corresponding to seasonal capital breeding (CN)—the trajectory will tend to that point. In figure 5*E*, adult starvation does not occur because adults have a sufficiently high intake rate.

Figure 5*F* illustrates bistability with adult starvation (BS). The red area represents reproductive strategies with seasonal income breeding with adult starvation (IS). Because having a nominal starting time before the nonstarvation period does not change the realized starting time of reproduction, and, likewise, because extending the nominal duration of the reproduction period beyond the nonstarvation period does not change the realized ending time of reproduction, for the reason that adults are not able to reproduce when starving, there is a range of evolutionarily neutral reproductive strategies that all lead to the same realized reproduction period, with the latter being identical to the nonstarvation period of adults. In the situation illustrated in figure 5*F*, the red area is locally evolutionarily attracting. Under such conditions, when the initial reproductive strategy is close to the red area, the evolutionary trajectory converges to it, resulting in seasonal income breeding with adult starvation (IS). Otherwise, trajectories tend to the evolutionary endpoint indicated by the orange circle, corresponding to seasonal capital breeding with adult starvation (CS).

Importantly, figure 5 reveals a clear difference in directional selection pressures and hence evolutionary timescales: the evolutionary trajectories rapidly converge to a one-dimensional manifold along which evolution then proceeds more slowly toward the evolutionary end point. This means that near the evolutionary end points, evolution proceeds in an essentially one-dimensional trait space, in which the considered variance-covariance matrix does not affect the convergence stability of the evolutionary end points. Therefore, if the variance covariance matrices are not close to singular, the evolutionary end points and their convergence stability are independent of the considered evolutionary framework—adaptive dynamics theory or quantitative genetics theory—and of the elements of the considered variance-covariance matrices.

Now that we have described the different reproduction modes that can evolutionarily emerge, we next elaborate on the ecological conditions under which they occur.

### *Capital Breeding Evolves When Resource Availability Is Strongly Seasonal and Adults Are More Efficient Foragers than Juveniles*

The seasonality in resource growth rate is most significant when the oscillation amplitude $\omega$ is large and the peak width $\alpha$ is intermediate. If the peak width is large, the peak stretches across the whole seasonal cycle, implying high growth rates for most of the time. Similarly, when the peak width is small, the resource availability is also not strongly seasonal: in that case, the resource growth rate remains low most of the time, and the short duration of high growth rates does not strongly affect resource levels.

Figure 6 illustrates that seasonal capital breeding (blue region; CN or CS) evolves when resource availability is strongly seasonal and adults are more efficient resource foragers than juveniles. In contrast, income breeding (red region; IN or IS) evolves when resource availability is not strongly seasonal or when juveniles are more efficient resource foragers than adults. At the interface of these regions, evolutionary bistability arises between the two reproduction modes (purple region; BN, BS).

Figure 7*A* (see also fig. C1*B*) illustrates that around the BN region, where income-breeding strategies and capital-breeding strategies without adult starvation overlap, the duration of the reproduction period under seasonal capital breeding ($r_{\text{duration}} \approx 0.5$) significantly differs from that under continuous income breeding ($r_{\text{duration}} = 1$). Further away from this region—that is, where either the adult-juvenile intake ratio $\theta$ or the oscillation amplitude $\omega$ are larger—capital-breeding strategies become even more seasonal, having a shorter reproduction period. As a result, adults use more time for storing energy, and therefore we observe an increase in the proportion of offspring produced from capital breeding (fig. C1*C*). Biologically, when the seasonality in resource growth is significant, efficiently foraging adults need to time their reproduction so that the less efficiently foraging newborn juvenile individuals can experience sufficiently good resource conditions, and more juveniles can thus mature to the adult stage.

### *Seasonal Income Breeding Evolves When Juveniles Are More Efficient Foragers than Adults*

As shown by figure 6, it is primarily the seasonality in the resource growth rate and the relative intake efficiencies of juveniles and adults in the consumer population that determine the evolutionary outcomes in reproduction mode. The most important finding regarding the latter dependence is that seasonal income breeding (dark red region in fig. 6; IS) evolves when juveniles are more efficient foragers, that is, for small values of the adult-juvenile intake ratio $\theta$. Under these conditions, it is beneficial for adults to reproduce whenever they can (i.e., when they are not starving), as their juvenile offspring can forage on the resource at a higher mass-specific rate.

Figure C1*A* shows that the transition from continuous income breeding (IN) to seasonal income breeding (IS)

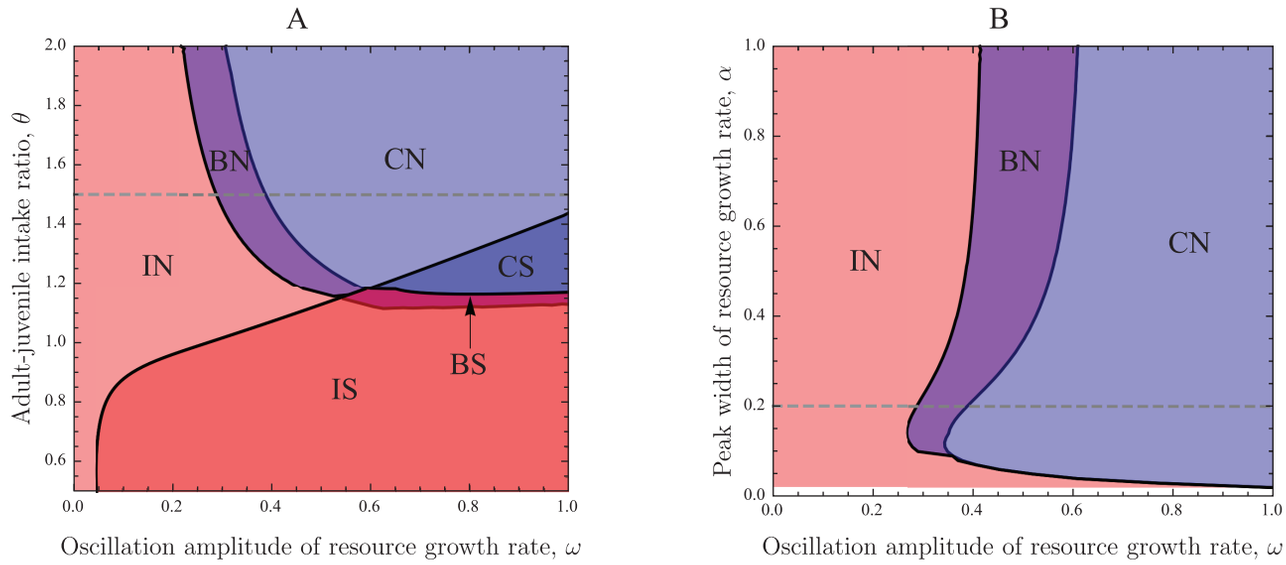


**Figure 6:** Capital breeding evolves when resource availability is strongly seasonal and adults are more efficient foragers than juveniles. The labeled parameter regions indicate the reproduction modes that result from evolution of the reproductive strategy, depending on the oscillation amplitude $\omega$ and the adult-juvenile intake ratio $\theta$ (*A*) and depending on the oscillation amplitude $\omega$ and the peak width $\alpha$ (*B*). The labels of the different regions have the same meanings as in figures 3–5. In both panels, evolution to income breeding (IN, IS) is indicated by red regions, evolution to capital breeding (CN, CS) is indicated by blue regions, and evolutionary bistability (BN, BS) between these reproduction modes is indicated by purple regions. In *A*, $\alpha = 0.2$, and in *B*, $\theta = 1.5$, as indicated by the horizontal dashed lines in the two panels. The bottom-right area of *A* corresponds to the parameter region in which adults starve during part of the season (IS, BS, and CS). All other parameters have the default values shown in table 1.

with changing adult-juvenile intake ratio $\theta$ is continuous. It also shows that when adults starve, decreasing the adult-juvenile intake ratio $\theta$ leads to a longer starvation period of adults, which for seasonal income breeding implies a shorter reproduction period.

### *Transitions between Income Breeding and Capital Breeding Are Not Smooth, Involving Evolutionary Bistabilities and Abrupt Changes of Reproduction Periods*

Figure 7 illustrates how the transitions between the different reproduction modes occur. Since the starvation periods are not completely independent of the reproductive strategy, we plot the starvation periods corresponding to the evolutionary outcomes. In the regions labeled BN and BS, evolutionary bistability occurs and we have chosen to show the starvation periods for the income-breeding strategy. Figure 7*A* illustrates the transition from capital breeding (CN) to income breeding (IN) when adults are not starving, as resulting from decreasing the oscillation amplitude $\omega$ of the resource growth rate. Analogously, figure 7*B* illustrates the transition from seasonal capital breeding with no adult starvation (CN) to seasonal income breeding with adult starvation (IS), as resulting from decreasing the adult-juvenile intake ratio $\theta$. The latter change could be driven, for example, by an imposed gradual change in the diet composition of the consumer population. Figure C2 shows the transitions resulting from changing the peak width $\alpha$ of the resource growth rate and from changing the adult-juvenile intake ratio $\theta$ for another value of the oscillation amplitude $\omega$.

Figure 7 shows that transitions between income breeding (IN) and capital breeding (CN and CS) are not continuous; that is, the income-breeding strategy does not continuously change into a capital-breeding strategy when the seasonality in resource availability becomes more pronounced. Instead, for intermediate parameter ranges, there is evolutionary bistability, so that the evolutionary outcome depends on the initial reproductive strategy. This is associated with an evolutionary hysteresis pattern: starting from income breeding (IN), the income-breeding strategy prevails through the parameter region with evolutionary bistability (BN) and suddenly evolves to capital breeding (CN) when the evolutionary bistability ends. In the opposite direction, the same pattern applies: starting from capital breeding (CN), the capital-breeding strategy prevails through the parameter region with evolutionary bistability (BN) and suddenly evolves to income breeding (IN) when the evolutionary bistability ends.

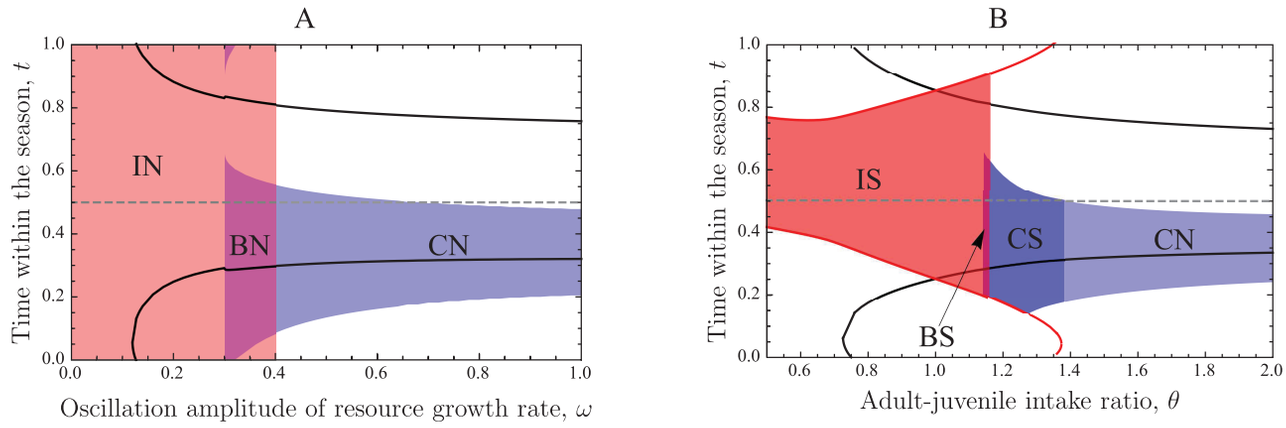


**Figure 7:** Abrupt transitions from income breeding to capital breeding. Reproduction periods and starvation periods are shown as functions of the oscillation amplitude $\omega$ (*A*) and the adult-juvenile intake ratio $\theta$ (*B*). The reproduction periods are depicted as color-filled areas (red = income breeding; blue = capital breeding), with the reproduction modes indicated by the labels used in figure 6. The boundaries of the starvation periods are depicted by lines (black = juvenile starvation; red = adult starvation). Note that in *A*, although the purple BN region appears to consist of two separate regions, it is actually one connected region extending over the periodic boundary (as in the example shown in fig. 2*A*). The horizontal dashed lines show the peak of the resource growth rate at $t = 0.5$. In *A*, $\theta = 1.5$ and $\alpha = 0.2$, while in *B*, $\omega = 0.9$ and $\alpha = 0.2$. All other parameters have the default values shown in table 1.

### *Seasonal Capital Breeding Begins Already before Juveniles Experience Good Resource Availability*

Figure 7 also shows that for seasonal capital breeding (CN in fig. 7*A* and 7*B* and CS in fig. 7*B*), reproduction begins already before the resource availability reaches a level at which juveniles are not starving (as evidenced by the parts of the blue regions lying below the lower black line in fig. 7). This means that at the beginning of each reproduction period, newborn offspring are experiencing starvation with corresponding mortality. On the one hand, the resource availability is not sufficient for all newborn offspring to mature, while on the other hand, the newborn offspring need sufficient time to grow in body size. The reproductive strategy at the evolutionary outcome thus represents a compromise between the amount of offspring that can survive until a good resource level is available and the time within the season remaining for them to grow in body size.

## Discussion

Environmental changes are expected to be drivers of evolutionary changes in phenology (Réale et al. 2003; Bradshaw and Holzapfel 2006). In this article, we have devised and analyzed a biomass-based stage-structured consumer-resource model to study the evolution of consumer reproductive strategies in seasonal environments. Contrary to earlier evolutionary models of reproductive phenology that have focused on only the starting time of reproduction (e.g., Iwasa and Levin 1995; Yamamura et al. 2007; Lindh et al. 2016), our model additionally allows for the duration of the reproduction period to evolve independently. We have focused on the effects of changing the seasonality of the environment through changing the temporal pattern of resource growth in terms of oscillation amplitude and peak width. On this basis, we have shown that changes in seasonal environments can have profound impacts on reproduction schedules, including qualitative and abrupt changes in reproduction mode. We have also shown that energetic asymmetry between the two consumer stages has a profound impact on the evolution of reproduction modes. Our analyses reveal a strong and decisive interaction between these two factors: capital-breeding strategies evolve when adults have a much higher mass-specific intake rate than juveniles and the seasonality in resource growth is sufficiently pronounced. Otherwise, income-breeding strategies (either seasonal or continuous) evolve. Finally, as shown in figure 6, transitions from income breeding to capital breeding and vice versa occur in an abrupt fashion, with evolutionary bistability occurring in the intermediate parameter ranges in which neither of these reproduction modes is sufficiently advantageous.

Our model assumes that juveniles and adults compete for the same resource but differ in their competitive abilities. Meeting this assumption usually requires that juveniles and adults share the same habitat and have overlapping generations, a common situation for many birds and mammals and, to some extent, for fish and hemimetabolous insects (Ebenman 1988; Cushing and Li 1992). We argue that the model can also provide evolutionary

insights for species in which premetamorphic juveniles (i.e., larvae) live in a different habitat than adults and postmetamorphic juveniles settle in the adult habitat and compete there with the adults: this applies to many amphibians, fish, and marine invertebrates. Furthermore, our model may also apply to size-dependent competition in plants (e.g., Lamb and Cahill 2006), provided that the growth of the limiting resource resembles semichemostat dynamics, which requires that the limiting resource is a nutrient rather than light.

Our results reveal how adult consumers adapt to changing environments by timing their reproduction. Compared with previous studies that focused on only the starting time of the reproduction periods, our model predicts several qualitatively different reproduction modes and their dependence on the strength of the seasonality of the environments. When the environment is aseasonal or only weakly seasonal, it does not matter when adults reproduce. With increasing seasonality, reproductive phenology starts to matter more and more. When the growth and maturation of juveniles are resource dependent, evolution does not favor adults that reproduce when the resource availability is low (e.g., during winter) because juvenile individuals are then confronted with starvation, and their growth and maturation will halt. Consequently, it is evolutionarily favorable for adults to store energy during winter (if they can) and reproduce when the resource availability starts to recover in spring (figs. 3, 4, 7). As a consequence, capital breeding is expected to evolve in significantly seasonal environments.

Seasonal variation in resource availability usually requires consumers to time their reproduction so that the resultant peak of resource demand is synchronized with the environment's peak of resource supply (Daan et al. 1989; Williams et al. 2014). Otherwise, a mismatch between demand and supply will reduce recruitment success (Visser et al. 1998; Durant et al. 2007; Knudsen et al. 2011). The aforementioned empirical studies show that reproduction usually starts before food availability peaks so as to ensure sufficient time for the offspring to grow. Our results are consistent with these studies, but we also show that reproductive strategies may evolve through which adults start reproducing already while resource availability is still so low that their offspring experience considerable additional mortality from starvation. More generally, adults attempt to time (at least a major part of) their reproduction periods before the peak of the resource growth rate (figs. 3, 4, 6) except under income breeding with adult starvation, in which case they have to reproduce whenever they are not starving.

Our model predicts that when seasonal variation in the environment gets more pronounced (increasing oscillation amplitude $\omega$), the reproduction strategy evolves from continuous to seasonal breeding (fig. 6). This prediction holds irrespective of whether adults or juveniles are the superior competitors and agrees with the prevalence of seasonal reproduction outside the lower latitudes. A more specific prediction is the switch from income breeding to capital breeding with increasing seasonality, provided that adults are better competitors than juveniles (fig. 6). Interspecific latitudinal gradients toward breeding increasingly relying on stored resources have been documented for crustaceans (Sainmont et al. 2014) and fish (McBride et al. 2015). Similarly, the common eider *Somateria mollissima*, probably the most extreme capital breeder among flying birds, is an Arctic breeder (Sénéchal et al. 2011). The pattern can also be observed within single species, as in the common frog *Rana temporaria* over a latitudinal gradient (Jönsson et al. 2009) and in the toad *Sclerophrys gutturalis*, where an invasive population established in a cooler climate than its native source adopted a more capital-based breeding strategy (Vimercati et al. 2019). Nevertheless, species classified as primarily income breeding do occur at high latitudes too—for example, the Antarctic fur seal *Arctocephalus gazella* (Boyd 2000) and the harlequin duck *Histrionicus histrionicus* (Bond et al. 2007)—suggesting that factors not included in our model can also be important.

Some earlier studies, such as those by Kooi and Troost (2006) and Fischer et al. (2010), have already proposed that energy storage can be advantageous in fluctuating environments. Our current study corroborates this prediction and reveals that the advantage of energy storage increases with the seasonality of environments. We extend the previous research by showing that the advantages of energy storage by adults are weakened and may even disappear, for example, when juveniles have a much higher efficiency of resource acquisition, in which case adults may attempt to reproduce when they are not starving. Accordingly, income-breeding strategies can evolve even when the seasonality of environments is significant (fig. 7*B*). Furthermore, we have shown that alternative evolutionary outcomes occur when income-breeding strategies and capital-breeding strategies both have the potential to evolve; such evolutionary bistability arises for intermediately seasonal environments.

Our results show that the adult-juvenile intake ratio is a key parameter affecting the evolution of reproductive strategies. This is in line with earlier studies showing that this parameter has profound consequences for population dynamics (de Roos et al. 2007; Guill 2009; Sun and de Roos 2017). The key distinction is whether adults are competitively superior to juveniles. For interspecific competition, larger individuals are typically competitively superior to smaller ones (Schoener 1983; Persson 1985), and the same pattern is often assumed to apply to intraspecific competition as well (Sutherland 1996).

However, while the competitive superiority of larger individuals is well established for cases involving interference competition (Persson 1985) as well as under intraspecific competition (e.g., Goss-Custard et al. 1982; Sol et al. 1998), the situation is less clear for exploitation competition (Persson 1985). Under intraspecific exploitation competition, small or intermediately sized individuals can be at an advantage, especially at low food levels (Persson et al. 1998; Claessen et al. 2000; Hjelm and Persson 2001; Aljetlawi and Leonardsson 2003). Thus, cases of adult and juvenile competitive superiority are both realistic and important to understand.

While all the processes involved in consumer population dynamics (development and maturation, reproduction and mortality) are resource dependent and are thus affected by environmental changes, the intake rate of adults relative to juveniles is not affected by environmental changes. This parameter affects the evolutionary outcomes because it determines which stage has the higher efficiency of resource utilization and thus indirectly determines the advantageousness of storing reproductive energy by adults. Most importantly, our results reveal that adults evolve to become income breeders when competition among them is stronger than among juveniles, for example, for small values of the adult-juvenile intake ratio. This is a rare case in which the phenology of the resource becomes irrelevant for the evolutionary outcome (fig. 6*A*).

A direct consequence of the energetic asymmetry is that it allows capital-breeding strategies to evolve only when the seasonality in resource growth is significant and only when adults are more efficient foragers than juveniles. More specifically, when the two consumer stages have the same resource intake rate, that is, when the adult-juvenile intake ratio equals 1, only income-breeding strategies can evolve (figs. 6*A*, 7*B*), even for large seasonal oscillations in resource growth. In figure 6*A*, we have mapped the degree of asymmetry allowing capital-breeding strategies to evolve. Another consequence of the energetic asymmetry is that it allows alternative evolutionary outcomes to occur for the same ecological settings. Similar to the aforementioned results regarding intermediately seasonal environments, evolutionary bistability occurs for intermediate values of the adult-juvenile intake ratio, at which the advantages of energy storage are not sufficiently significant.

We have shown that income-breeding strategies evolve when the seasonality in the resource growth rate is not too pronounced (i.e., for small oscillation amplitudes $\omega$ and sufficiently small peak widths $\alpha$ of the resource growth rate) and when the adult-juvenile intake ratio $\theta$ is small. Otherwise, capital-breeding strategies evolve, in which at least part of the reproduction of adults is financed by energy reserves stored during the nonreproduction periods. In our model, capital-breeding strategies are always mixed strategies involving the use of both stored energy and current intake, which is also common for capital breeding in the wild (Meijer and Drent 1999; Sénéchal et al. 2011). However, pure capital-breeding strategies are sometimes observed in the wild (Sénéchal et al. 2011; Sainmont et al. 2014): in these cases, adults do not feed while they are reproducing, so reproduction is financed entirely by energy reserves. In our model, this would require reproduction to take place only when adults are starving, which we have never observed as an evolutionary outcome. Even for capital breeding with adult starvation, reproduction occurs when adults are not starving (e.g., right column of fig. 4), which means that the intake of the resource directly contributes to reproduction. However, if the model assumption that adults are still consuming the resource during their reproduction periods is relaxed, or if juveniles and adults are assumed to feed on different resources, qualitatively different outcomes may be predicted. In particular, such assumptions could result in the evolution of pure capital-breeding strategies. This is because in our model, adults have to pay maintenance costs at all times, resulting in additional starvation mortality if they do not feed, which favors pure income-breeding strategies that attempt to release their energy reserves in a relatively short period.

Possible future extensions of this study include incorporating a trade-off between reproduction and survival in the adult stage. Our assumption that adults can use their net biomass gain only to reproduce results in evolutionary outcomes in which adults attempt to reproduce when they are not starving. It is suggested that many organisms face a trade-off between reproduction and somatic maintenance and thus survival, in particular when resource availability is limited (Flatt and Kawecki 2007), making this trade-off a fundamental ingredient of many evolutionary and ecological models (Roff 1992; Stearns 1992). Furthermore, in our current study, we have not considered any costs of energy storage, which may be important, at least in endotherms (Bonnet et al. 1998). Another extension is to consider a more striking seasonal pattern of resource fluctuations than the smooth pattern we have assumed; for example, the resource could be practically absent during parts of the year.

In summary, the evolution of an organism's reproduction period in a stage-structured consumer population can result in a rich array of outcomes, including seasonal and continuous reproduction, capital and income breeding, and evolutionary bistability in intermediate cases. Our research elucidates the evolution of reproductive strategies in changing environments and provides a framework for the further study of life-history evolution in more complex systems incorporating trade-offs between reproduction and survival and between reproduction and reproductive energy storage.

## Acknowledgments

This research was initiated during Z.S.'s participation in the Young Scientists Summer Program of the International Institute for Applied Systems Analysis (IIASA). Z.S. was financially supported by the Nederlandse Organisatie voor Wetenschappelijk Onderzoek (NWO) for the research at IIASA. Additionally, Z.S. is grateful for support by the China Scholarship Council. A.M.d.R. is supported by funding from the European Research Council (ERC) under the European Union's Seventh Framework Programme (FP/2007–2013)/ERC grant agreement 322814. J.A.J.M. benefited from support by the Chaire Modélisation Mathématique et Biodiversité, enabled by the cooperation of Veolia Environnement, the Ecole Polytechnique, the Museum National d'Histoire Naturelle, and Fondation X. Z.S., K.P., M.H., J.A.J.M., and U.D. gratefully acknowledge funding from the International Institute for Applied Systems Analysis (IIASA) and the National Member Organizations that support the institute.


## APPENDIX A

### Maturation Function

In this appendix, we show the juvenile maturation rate $\gamma(\nu, \delta)$ in equation (6) as a function of the net biomass productivity $\nu$ of juveniles (fig. A1). This function is continuous and smooth for positive $\nu$ and $\delta$ (also around $\nu \approx \delta$). Furthermore, $\gamma(\nu, \delta)$ tends to zero for $\nu \to 0^+$ (from the positive side, red circle in fig. A1) and to $-\delta/\ln(z)$ for $\nu \to \delta$ (blue circle in fig. A1). In our numerical calculations, when $\nu$ is sufficiently close to these values, $\gamma$ is thus set to 0 and $-\delta/\ln(z)$, respectively.

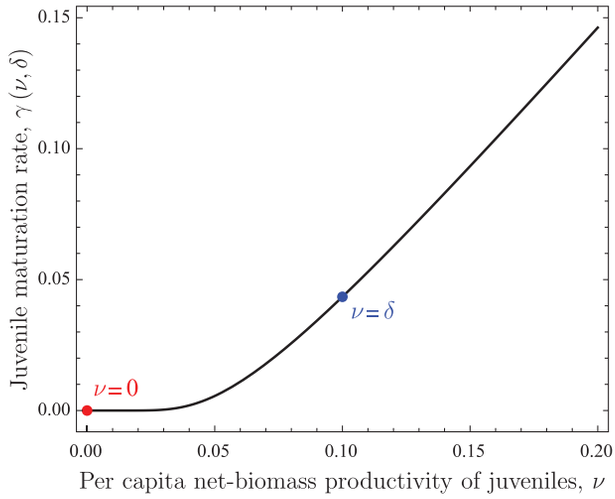


**Figure A1:** Dependence of the juvenile maturation rate $\gamma(\nu, \delta)$ on the per capita net biomass productivity $\nu$ of juveniles. All other parameters have the default values shown in table 1.

## APPENDIX B

### Invasion Fitness and Selection Gradient

In this appendix, we explain how to calculate the invasion fitness $F((r_{\text{start}}, r_{\text{duration}}), (r'_{\text{start}}, r'_{\text{duration}}))$ and the selection gradient $(g_{r_{\text{start}}}(r_{\text{start}}, r_{\text{duration}}), g_{r_{\text{duration}}}(r_{\text{start}}, r_{\text{duration}}))$. The invasion fitness is defined as the long-term exponential growth rate of rare variants with traits $(r'_{\text{start}}, r'_{\text{duration}})$ in the environment established by a resident population with traits $(r_{\text{start}}, r_{\text{duration}})$. The two components of the selection gradient are defined as

$$g_{r_{\text{start}}}(r_{\text{start}}, r_{\text{duration}}) = \left.\frac{\partial F((r_{\text{start}}, r_{\text{duration}}), (r'_{\text{start}}, r'_{\text{duration}}))}{\partial r'_{\text{start}}}\right|_{r'_{\text{start}} = r_{\text{start}}, r'_{\text{duration}} = r_{\text{duration}}},$$

$$g_{r_{\text{duration}}}(r_{\text{start}}, r_{\text{duration}}) = \left.\frac{\partial F((r_{\text{start}}, r_{\text{duration}}), (r'_{\text{start}}, r'_{\text{duration}}))}{\partial r'_{\text{duration}}}\right|_{r'_{\text{start}} = r_{\text{start}}, r'_{\text{duration}} = r_{\text{duration}}}.$$

In a first step, we integrate the resident population dynamics until an ecological attractor is reached. We denote the resultant time course of the resource density by $R(t)$. As this time course fully captures the impact of the resident traits $(r_{\text{start}}, r_{\text{duration}})$, which therefore are no longer in need of being made explicit, we denote (for the sake of notational simplicity) the traits of the rare variant by $(r_{\text{start}}, r_{\text{duration}})$ instead of $(r'_{\text{start}}, r'_{\text{duration}})$ throughout this appendix.

In a second step, we determine the 3-vectors

$$m_{\text{R}}(t) = (J(t), A(t), B_{\max}(t))^{\text{T}},$$
$$m_{\text{S}}(t) = (J(t), A(t), B(t))^{\text{T}},$$

describing the within-season dynamics of the rare variant's juvenile biomass density $J(t)$ and adult biomass density $A(t)$, with the variables $B_{\max}(t)$ and $B(t)$ describing energy storage. Here the subscripts R and S are labels corresponding to the two phases of the model dynamics: energy release (R) and energy storage (S). Since the resource-consumer system undergoes a stable cycle with period 1, it suffices to focus on the dynamics during one cycle period, from $t = r_{\text{start}}$ to $t = r_{\text{start}} + 1$. These dynamics are described by the following two ordinary differential equation systems:

$$\frac{\mathrm{d}m_{\text{R}}(t)}{\mathrm{d}t} = \mathbf{\Phi}_{\text{R}}(t, r_{\text{duration}}) m_{\text{R}}(t) \text{ for } t \in [r_{\text{start}}, r_{\text{start}} + r_{\text{duration}}], \tag{B1a}$$

$$\frac{\mathrm{d}m_{\mathrm{S}}(t)}{\mathrm{d}t} = \mathbf{\Phi}_{\mathbf{S}}(t)m_{\mathrm{S}}(t) \text{ for } t \in [r_{\mathrm{start}} + r_{\mathrm{duration}}, r_{\mathrm{start}} + 1], \tag{B1b}$$

where

$$\mathbf{\Phi}_{\mathbf{R}}(t, r_{\mathrm{duration}}) = \begin{pmatrix} \nu_{\mathrm{j}}(R(t)) - \gamma(\nu_{\mathrm{j}}^{+}(R(t)), \delta) - \delta & \nu_{\mathrm{a}}^{+}(R(t)) & \frac{1}{r_{\mathrm{duration}}} \\ \gamma(\nu_{\mathrm{j}}^{+}(R(t)), \delta) & -d_{\mathrm{a}}(R(t)) & 0 \\ 0 & 0 & -d_{\mathrm{a}}(R(t)) \end{pmatrix} \tag{B1c}$$

and analogously

$$\mathbf{\Phi}_{\mathbf{S}}(t) = \begin{pmatrix} \nu_{\mathrm{j}}(R(t)) - \gamma(\nu_{\mathrm{j}}^{+}(R(t)), \delta) - \delta & 0 & 0 \\ \gamma(\nu_{\mathrm{j}}^{+}(R(t)), \delta) & -d_{\mathrm{a}}(R(t)) & 0 \\ 0 & \nu_{\mathrm{a}}^{+}(R(t)) & -d_{\mathrm{a}}(R(t)) \end{pmatrix}. \tag{B1d}$$

In a third step, we determine the next-season matrix by integrating the rare variant's dynamics over one season. The rarity of the variants means that they cause and experience no density dependence within their own subpopulation. Accordingly, the population dynamics of the rare variants are linear, described by a next-season matrix. For this reason, the dynamics of $m(t)$ for any initial condition is fully known from the dynamics of $m(t)$ for initial conditions given by the three unit vectors. We therefore integrate the ordinary differential equation system in equation (B1a) over the time interval $t \in [r_{\mathrm{start}}, r_{\mathrm{start}} + r_{\mathrm{duration}}]$ using three different groups of initial conditions, which we denote by $m_{\mathrm{RJ}}(r_{\mathrm{start}}) = (1, 0, 0)^{\mathrm{T}}$, $m_{\mathrm{RA}}(r_{\mathrm{start}}) = (0, 1, 0)^{\mathrm{T}}$, and $m_{\mathrm{RB}}(r_{\mathrm{start}}) = (0, 0, 1)^{\mathrm{T}}$, leading to three different groups of final values, which we collect in a matrix:

$$\mathbf{M}_{\mathbf{R}}(r_{\mathrm{start}} + r_{\mathrm{duration}}) = (m_{\mathrm{RJ}}(r_{\mathrm{start}} + r_{\mathrm{duration}}), m_{\mathrm{RA}}(r_{\mathrm{start}} + r_{\mathrm{duration}}), m_{\mathrm{RB}}(r_{\mathrm{start}} + r_{\mathrm{duration}})). \tag{B2a}$$

Analogously, we integrate the ordinary differential equation system in equation (B1b) over the time interval $t \in [r_{\mathrm{start}} + r_{\mathrm{duration}}, r_{\mathrm{start}} + 1]$ using three different groups of initial values, which we denote by $m_{\mathrm{SJ}}(r_{\mathrm{start}} + r_{\mathrm{duration}}) = (1, 0, 0)^{\mathrm{T}}$, $m_{\mathrm{SA}}(r_{\mathrm{start}} + r_{\mathrm{duration}}) = (0, 1, 0)^{\mathrm{T}}$, and $m_{\mathrm{SB}}(r_{\mathrm{start}} + r_{\mathrm{duration}}) = (0, 0, 1)^{\mathrm{T}}$, leading to three different groups of final values, which we again collect in a matrix:

$$\mathbf{M}_{\mathbf{S}}(r_{\mathrm{start}} + 1) = (m_{\mathrm{SJ}}(r_{\mathrm{start}} + 1), m_{\mathrm{SA}}(r_{\mathrm{start}} + 1), m_{\mathrm{SB}}(r_{\mathrm{start}} + 1)). \tag{B2b}$$

The six vectors $m_{\mathrm{RJ}}(r_{\mathrm{start}} + r_{\mathrm{duration}})$, $m_{\mathrm{RA}}(r_{\mathrm{start}} + r_{\mathrm{duration}})$, $m_{\mathrm{RB}}(r_{\mathrm{start}} + r_{\mathrm{duration}})$, $m_{\mathrm{SJ}}(r_{\mathrm{start}} + 1)$, $m_{\mathrm{SA}}(r_{\mathrm{start}} + 1)$, and $m_{\mathrm{SB}}(r_{\mathrm{start}} + 1)$ are all column 3-vectors, so $\mathbf{M}_{\mathbf{R}}(r_{\mathrm{start}} + r_{\mathrm{duration}})$ and $\mathbf{M}_{\mathbf{S}}(r_{\mathrm{start}} + 1)$ are $3 \times 3$ matrices.

The last row of the matrix $\mathbf{M}_{\mathbf{R}}(r_{\mathrm{start}} + r_{\mathrm{duration}})$ contains values of $B_{\max}(r_{\mathrm{start}} + r_{\mathrm{duration}})$, not $B(r_{\mathrm{start}} + r_{\mathrm{duration}}) = 0$, which is the actual amount of storage at the end of the reproduction period according to equation (8d). Because only $J$ and $A$ thus differ from zero at the end of the reproduction period, we need to take only the first two rows of $\mathbf{M}_{\mathbf{R}}(r_{\mathrm{start}} + r_{\mathrm{duration}})$ when calculating the next-season matrix; we denote this submatrix as $\mathbf{M}_{\mathbf{R}}^{*}(r_{\mathrm{start}} + r_{\mathrm{duration}})$. Furthermore, at the end of the nonreproduction period, $B$ can differ from zero but not at its beginning. Accordingly, we need to take only the first two columns of $\mathbf{M}_{\mathbf{S}}(r_{\mathrm{start}} + 1)$ when calculating the next-season matrix; we denote this submatrix as $\mathbf{M}_{\mathbf{S}}^{*}(r_{\mathrm{start}} + 1)$. Hence, the values $m_{\mathrm{SB}}(r_{\mathrm{start}} + 1)$ with initial conditions $m_{\mathrm{SB}}(r_{\mathrm{start}} + r_{\mathrm{duration}}) = (0, 0, 1)^{\mathrm{T}}$ need not be calculated. The next-season matrix is thus given by the $2 \times 2$ matrix

$$\boldsymbol{\mathcal{M}}(r_{\mathrm{start}}, r_{\mathrm{duration}}) = \mathbf{M}_{\mathbf{R}}^{*}(r_{\mathrm{start}} + r_{\mathrm{duration}})\mathbf{M}_{\mathbf{S}}^{*}(r_{\mathrm{start}} + 1),$$

and the invasion fitness is its dominant eigenvalue.

In a fourth step, we determine the derivatives of the next-season matrix with respect to the two traits, as these derivatives are needed for calculating the selection gradient. We first consider the derivative of $\boldsymbol{\mathcal{M}}(r_{\mathrm{start}}, r_{\mathrm{duration}})$ with respect to $r_{\mathrm{start}}$. The derivative of $\mathbf{M}_{\mathbf{R}}(r_{\mathrm{start}} + r_{\mathrm{duration}})$ with respect to $r_{\mathrm{start}}$ is

$$\frac{\partial \mathbf{M}_{\mathbf{R}}(r_{\mathrm{start}} + r_{\mathrm{duration}})}{\partial r_{\mathrm{start}}} = -\mathbf{M}_{\mathbf{R}}(r_{\mathrm{start}} + r_{\mathrm{duration}})\mathbf{\Phi}_{\mathbf{R}}(r_{\mathrm{start}}, r_{\mathrm{duration}}) + \mathbf{\Phi}_{\mathbf{R}}(r_{\mathrm{start}} + r_{\mathrm{duration}}, r_{\mathrm{duration}})\mathbf{M}_{\mathbf{R}}(r_{\mathrm{start}} + r_{\mathrm{duration}}). \tag{B3a}$$

Analogously, the derivative of $\mathbf{M}_{\mathbf{S}}(r_{\mathrm{start}} + 1)$ with respect to $r_{\mathrm{start}}$ is

$$\frac{\partial \mathbf{M}_{\mathbf{S}}(r_{\mathrm{start}} + 1)}{\partial r_{\mathrm{start}}} = -\mathbf{M}_{\mathbf{S}}(r_{\mathrm{start}} + 1)\mathbf{\Phi}_{\mathbf{S}}(r_{\mathrm{start}} + r_{\mathrm{duration}}) + \mathbf{\Phi}_{\mathbf{S}}(r_{\mathrm{start}} + 1)\mathbf{M}_{\mathbf{S}}(r_{\mathrm{start}} + 1). \tag{B3b}$$

We denote by $\partial \mathbf{M}_{\mathbf{R}}^{*}(r_{\mathrm{start}} + r_{\mathrm{duration}})/\partial r_{\mathrm{start}}$ the $2 \times 3$ matrix consisting of the first two rows of $\partial \mathbf{M}_{\mathbf{R}}(r_{\mathrm{start}} + r_{\mathrm{duration}})/\partial r_{\mathrm{start}}$. Analogously, we denote by $\partial \mathbf{M}_{\mathbf{S}}^{*}(r_{\mathrm{start}} + 1)/\partial r_{\mathrm{start}}$ the $3 \times 2$ matrix consisting of the first two columns of $\partial \mathbf{M}_{\mathbf{S}}(r_{\mathrm{start}} + 1)/\partial r_{\mathrm{start}}$. Using the results above, the derivative of $\boldsymbol{\mathcal{M}}(r_{\mathrm{start}}, r_{\mathrm{duration}})$ with respect to $r_{\mathrm{start}}$ is given by

$$\frac{\partial \mathcal{M}(r_{\text{start}}, r_{\text{duration}})}{\partial r_{\text{start}}} = \frac{\partial \mathbf{M}_{\mathbf{R}}^{*}(r_{\text{start}} + r_{\text{duration}})}{\partial r_{\text{start}}} \mathbf{M}_{\mathbf{S}}^{*}(r_{\text{start}} + 1) + \mathbf{M}_{\mathbf{R}}^{*}(r_{\text{start}} + r_{\text{duration}}) \frac{\partial \mathbf{M}_{\mathbf{S}}^{*}(r_{\text{start}} + 1)}{\partial r_{\text{start}}}. \tag{B3c}$$

We next consider the derivative of $\mathcal{M}(r_{\text{start}}, r_{\text{duration}})$ with respect to $r_{\text{duration}}$. The derivative of $\mathbf{M}_{\mathbf{S}}(r_{\text{start}} + 1)$ with respect to $r_{\text{duration}}$ is

$$\frac{\partial \mathbf{M}_{\mathbf{S}}(r_{\text{start}} + 1)}{\partial r_{\text{duration}}} = -\mathbf{M}_{\mathbf{S}}(r_{\text{start}} + 1)\mathbf{\Phi}_{\mathbf{S}}(r_{\text{start}} + r_{\text{duration}}). \tag{B4a}$$

Since the duration $r_{\text{duration}}$ affects not only the duration of the reproduction period but also the speed at which stored energy is released during the reproduction period, to calculate the derivative of $\mathbf{M}_{\mathbf{R}}(r_{\text{start}} + r_{\text{duration}})$ with respect to $r_{\text{duration}}$, we need to solve two additional equations together with equation (B1a):

$$\frac{\mathrm{d}\tilde{J}(t)}{\mathrm{d}t} = (\nu_{\text{j}}(R) - \gamma(\nu_{\text{j}}^{+}(R), \delta) - \delta)\tilde{J}(t) + \nu_{\text{a}}^{+}(R)\tilde{A}(t) - \frac{B_{\max}(t)}{r_{\text{duration}}^{2}}, \tag{B4b}$$

$$\frac{\mathrm{d}\tilde{A}(t)}{\mathrm{d}t} = \gamma(\nu_{\text{j}}^{+}(R), \mu)\tilde{J}(t) - d_{\text{a}}(R)\tilde{A}(t), \tag{B4c}$$

where $\tilde{J}(t) = \partial J(t)/\partial r_{\text{duration}}$, $\tilde{A}(t) = \partial A(t)/\partial r_{\text{duration}}$, and $\tilde{J}(r_{\text{start}}) = \tilde{A}(r_{\text{start}}) = 0$. Akin to before, we denote by $\tilde{J}_i(r_{\text{start}} + r_{\text{duration}})$ and $\tilde{A}_i(r_{\text{start}} + r_{\text{duration}})$ with $i = J, A, B$ the final values for the three different groups of initial conditions corresponding to the three unit vectors $(1, 0, 0)^{\text{T}}$, $(0, 1, 0)^{\text{T}}$, and $(0, 0, 1)^{\text{T}}$, and we collect these solutions in a matrix:

$$\tilde{\mathbf{M}}_{\mathbf{R}}(r_{\text{start}} + r_{\text{duration}}) = \begin{pmatrix} \tilde{J}_{\text{J}}(r_{\text{start}} + r_{\text{duration}}) & \tilde{J}_{\text{A}}(r_{\text{start}} + r_{\text{duration}}) & \tilde{J}_{\text{B}}(r_{\text{start}} + r_{\text{duration}}) \\ \tilde{A}_{\text{J}}(r_{\text{start}} + r_{\text{duration}}) & \tilde{A}_{\text{A}}(r_{\text{start}} + r_{\text{duration}}) & \tilde{A}_{\text{B}}(r_{\text{start}} + r_{\text{duration}}) \\ 0 & 0 & 0 \end{pmatrix}. \tag{B4d}$$

We use this matrix to determine the derivative of $\mathbf{M}_{\mathbf{R}}(r_{\text{start}} + r_{\text{duration}})$ with respect to $r_{\text{duration}}$ as

$$\frac{\partial \mathbf{M}_{\mathbf{R}}(r_{\text{start}} + r_{\text{duration}})}{\partial r_{\text{duration}}} = \mathbf{\Phi}_{\mathbf{R}}(r_{\text{start}} + r_{\text{duration}}, r_{\text{duration}})\mathbf{M}_{\mathbf{R}}(r_{\text{start}} + r_{\text{duration}}) + \tilde{\mathbf{M}}_{\mathbf{R}}(r_{\text{start}} + r_{\text{duration}}). \tag{B4e}$$

Using the results above, the derivative of $\mathcal{M}(r_{\text{start}}, r_{\text{duration}})$ with respect to $r_{\text{duration}}$ is given by

$$\frac{\partial \mathcal{M}(r_{\text{start}} + r_{\text{duration}})}{\partial r_{\text{duration}}} = \frac{\partial \mathbf{M}_{\mathbf{R}}^{*}(r_{\text{start}} + r_{\text{duration}})}{\partial r_{\text{duration}}} \mathbf{M}_{\mathbf{S}}^{*}(r_{\text{start}} + 1) + \mathbf{M}_{\mathbf{R}}^{*}(r_{\text{start}} + r_{\text{duration}}) \frac{\partial \mathbf{M}_{\mathbf{S}}^{*}(r_{\text{start}} + 1)}{\partial r_{\text{duration}}}, \tag{B4f}$$

where we, akin to before, denote by $\partial \mathbf{M}_{\mathbf{R}}^{*}(r_{\text{start}} + r_{\text{duration}})/\partial r_{\text{duration}}$ the $2 \times 3$ matrix consisting of the first two rows of $\partial \mathbf{M}_{\mathbf{R}}(r_{\text{start}} + r_{\text{duration}})/\partial r_{\text{duration}}$ and by $\partial \mathbf{M}_{\mathbf{S}}^{*}(r_{\text{start}} + 1)/\partial r_{\text{duration}}$ the $3 \times 2$ matrix consisting of the first two columns of $\partial \mathbf{M}_{\mathbf{S}}(r_{\text{start}} + 1)/\partial r_{\text{duration}}$.

In a fifth step, we use the derivatives thus derived to calculate the selection gradient. With $\chi_{\text{L}}$ and $\chi_{\text{R}}$ denoting the left and right eigenvectors, respectively, of the next-season matrix $\mathcal{M}(r_{\text{start}}, r_{\text{duration}})$, the two components of the selection gradient

$$g(r_{\text{start}}, r_{\text{duration}}) = (g_{r_{\text{start}}}(r_{\text{start}}, r_{\text{duration}}), g_{r_{\text{duration}}}(r_{\text{start}}, r_{\text{duration}}))$$

are obtained as

$$g_{r_{\text{start}}}(r_{\text{start}}, r_{\text{duration}}) = \frac{\chi_{\text{L}}(\partial \mathcal{M}(r_{\text{start}}, r_{\text{duration}})/\partial r_{\text{start}})\chi_{\text{R}}}{\chi_{\text{L}}\chi_{\text{R}}}, \tag{B5a}$$

$$g_{r_{\text{duration}}}(r_{\text{start}}, r_{\text{duration}}) = \frac{\chi_{\text{L}}(\partial \mathcal{M}(r_{\text{start}}, r_{\text{duration}})/\partial r_{\text{duration}})\chi_{\text{R}}}{\chi_{\text{L}}\chi_{\text{R}}}, \tag{B5b}$$

where the derivatives of the next-season matrix are inserted according to equations (B3c) and (B4f). Indeed, no explicit expression of the selection gradient can be given. Because of seasonally varying growth conditions, juveniles and adults present at different times of the season have different expected amounts of descendants. Therefore, the left eigenvectors cannot easily be interpreted in terms of reproductive values. Extending the reproductive-value approach to infinitely many birth states (structured by time within the season) is beyond the scope of this study.

## APPENDIX C

### Additional Figures

#### *Quantitative Effects of Oscillation Amplitude and Adult-Juvenile Intake Ratio*

Complementing figure 6*A*, here we show three heat maps illustrating the quantitative effects of the oscillation amplitude $\omega$ of the resource growth rate and the adult-juvenile intake ratio $\theta$. Figure C1*A* shows the duration of the nonstarvation period of adults, which is, in the IS area, identical to the duration of the reproduction period; in

the IN, BN, and CN areas, there is no adult starvation, so the duration of the nonstarvation period is 1. Figure C1*B* shows the duration of the reproduction period for capital breeding, indicating the evolutionary endpoints. Figure C1*C* shows the proportion of capital breeding during the reproduction period, that is, the fraction

$$\frac{B(r_{\text{start}})/A(r_{\text{start}})}{B(r_{\text{start}})/A(r_{\text{start}}) + \int_{r_{\text{start}}}^{r_{\text{start}}+r_{\text{duration}}} \nu_a^+(R(t))\mathrm{d}t},$$

where $r_{\text{start}}$ and $r_{\text{duration}}$ are at the evolutionary endpoints.

### *Alternative Transition from Capital Breeding to Income Breeding*

Complementing figure 7, here we show two more panels illustrating the within-season timing. Figure C2*A* illustrates the transition from capital breeding (CN) to income breeding (IN) through decreasing the peak width $\alpha$ of the resource growth rate. This figure, together with figure 7*A*, makes it clear that seasonal capital breeding evolves for large values of the oscillation amplitude $\omega$ of the resource growth rate and intermediate values of $\alpha$.

Figure C2*B* illustrates another transition from capital breeding with no adult starvation (CN) to income breeding with adult starvation (IS) through decreasing the adult-juvenile intake ratio $\theta$. Unlike figure 7*B*, where the transition sequence is CN → CS → BS → IS (from left to right), here the transition sequence is CN → BN → IN → IS.

Figure C2 underscores that for seasonal capital breeding adults start reproducing already before their newborn offspring experience good resource availability as juveniles. The reason for this is explained in the main text.

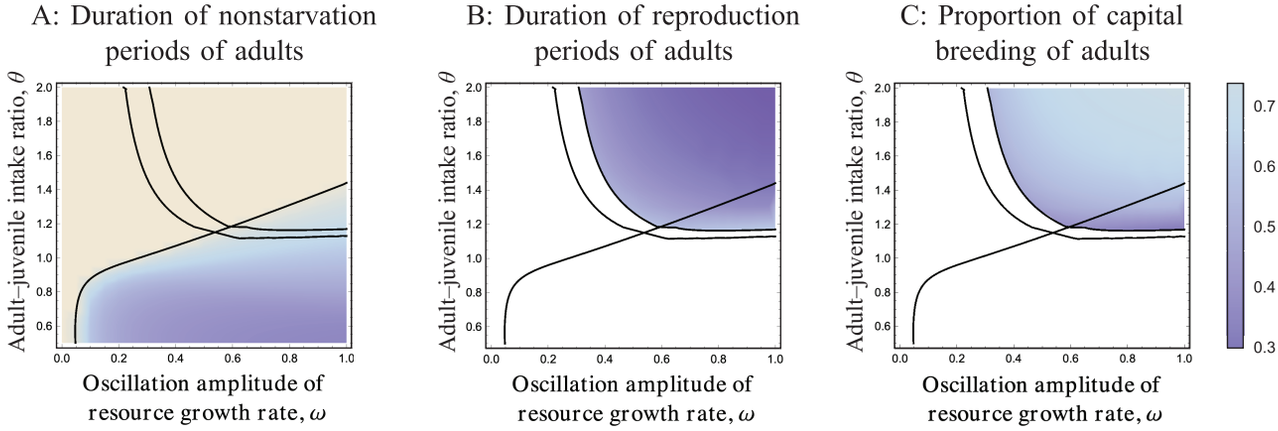


**Figure C1:** Quantitative effects of oscillation amplitude $\omega$ and adult-juvenile intake ratio $\theta$. *A*, Duration of the nonstarvation period of adults. *B*, Duration of the reproduction period of adults for capital-breeding strategies. *C*, Proportion of capital breeding during the reproduction period. All other parameters have the same values as in figure 6*A*.

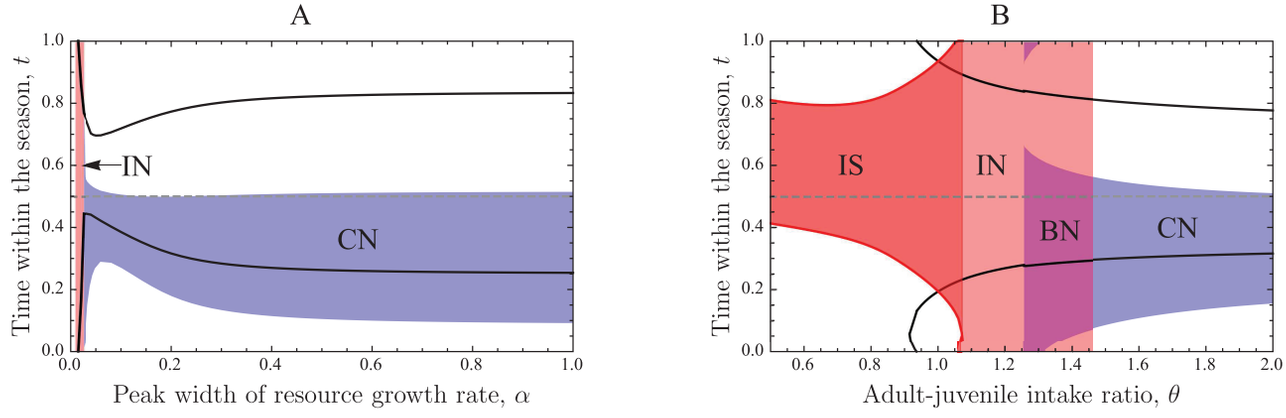


**Figure C2:** Alternative transition from capital breeding to income breeding. In *A*, $\theta = 1.5$ and $\omega = 0.7$, while in *B*, $\omega = 0.4$ and $\alpha = 0.2$. All other parameters have the default values shown in table 1.

## Literature Cited


Aljetlawi, A. A., and K. Leonardsson. 2003. Survival during adverse seasons reveals size-dependent competitive ability in a deposit-feeding amphipod, *Monoporeia affinis*. Oikos 101:164–170. https://doi.org/10.1034/j.1600-0706.2003.12183.x.

Altermatt, F. 2010. Tell me what you eat and I'll tell you when you fly: diet can predict phonological changes in response to climate change. Ecology Letters 13:1474–1484. https://doi.org/10.1111/j.1461-0248.2010.01534.x.

Bond, J. C., D. Esler, and K. Hobson. 2007. Isotopic evidence for sources of nutrients allocated to clutch formation by harlequin ducks. Condor 109:698–704. https://doi.org/10.1650/8241.1.

Bonnet, X., D. Bradshaw, and R. Shine. 1998. Capital versus income breeding: an ectothermic perspective. Oikos 83:333–342. https://doi.org/10.2307/3546846.

Boyd, I. L. 2000. State-dependent fertility in pinnipeds: contrasting capital and income breeders. Functional Ecology 14:623–630. https://doi.org/10.1046/j.1365-2435.2000.t01-1-00463.x.

Bradshaw, W. E., and C. M. Holzapfel. 2006. Evolutionary response to rapid climate change. Science 312:1477–1478. https://doi.org/10.1126/science.1127000.

Caswell, H. 2001. Matrix population models: construction, analysis, and interpretation. 2nd ed. Sinauer, Sunderland, MA.

Chuine, I., P. Yiou, N. Viovy, B. Seguin, V. Daux, and E. L. R. Ladurie. 2004. Grape ripening as a past climate indicator. Nature 432:289–290. https://doi.org/10.1038/432289a.

Claessen, D., A. M. de Roos, and L. Persson. 2000. Dwarfs and giants: cannibalism and competition in size-structured populations. American Naturalist 155:219–237. https://doi.org/10.1086/303315.

Cleland, E. E., N. R. Chiariello, S. R. Loarie, H. A. Mooney, and C. B. Field. 2006. Diverse responses of phenology to global changes in a grassland ecosystem. Proceedings of the National Academy of Sciences of the USA 103:13740–13744. https://doi.org/10.1073/pnas.0600815103.

Cushing, D. H. 1969. The regularity of the spawning season of some fish species. Journal du Conseil International pour l'Exploration de la Mer 33:81–92. https://doi.org/10.1093/icesjms/33.1.81.

Cushing, J. M., and J. Li. 1992. Intra-specific competition and density dependent juvenile growth. Bulletin of Mathematical Biology 54:503–519. https://doi.org/10.1007/BF02459632.

Daan, S., C. Dijkstra, R. Drent, and T. Meijer. 1989. Food supply and the annual timing of avian reproduction. Pages 392–407 *in* H. Ouellet, ed. Acta XIX Congressus Internationalis Ornithologici. Vol. 1. Proceedings of the XIX International Ornithological Congress. University of Ottawa Press, Ottawa.

de Roos, A. M., J. A. J. Metz, and L. Persson. 2013. Ontogenetic symmetry and asymmetry in energetics. Journal of Mathematical Biology 66:889–914. https://doi.org/10.1007/s00285-012-0583-0.

de Roos, A. M., T. Schellekens, T. van Kooten, K. van de Wolfshaar, D. Claessen, and L. Persson. 2007. Food-dependent growth leads to overcompensation in stage-specific biomass when mortality increases: the influence of maturation versus reproduction regulation. American Naturalist 170:E59–E76. https://doi.org/10.1086/520119.

———. 2008. Simplifying a physiologically structured population model to a stage-structured biomass model. Theoretical Population Biology 73:47–62. https://doi.org/10.1016/j.tpb.2007.09.004.

Dieckmann, U., and R. Law. 1996. The dynamical theory of coevolution: a derivation from stochastic ecological processes. Journal of Mathematical Biology 34:579–612. https://doi.org/10.1007/BF02409751.

Durant, J. M., D. Ø. Hjermann, G. Ottersen, and N. C. Stenseth. 2007. Climate and the match or mismatch between predator requirements and resource availability. Climate Research 33:271–283. https://doi.org/10.3354/cr033271.

Ebenman, B. 1988. Competition between age classes and population dynamics. Journal of Theoretical Biology 131:389–400. https://doi.org/10.1016/S0022-5193(88)80036-5.

Edwards, M., and A. J. Richardson. 2004. Impact of climate change on marine pelagic phenology and trophic mismatch. Nature 430:881–884. https://doi.org/10.1038/nature02808.

Fischer, B., U. Dieckmann, and B. Taborsky. 2010. When to store energy in a stochastic environment. Evolution 65:1221–1232. https://doi.org/10.1111/j.1558-5646.2010.01198.x.

Flatt, T., and T. J. Kawecki. 2007. Juvenile hormone as a regulator of the trade-off between reproduction and life span in *Drosophila melanogaster*. Evolution 61:1980–1991. https://doi.org/10.1111/j.1558-5646.2007.00151.x.

Geritz, S. A. H., E. Kisdi, G. Meszéna, and J. A. J. Metz. 1998. Evolutionarily singular strategies and the adaptive growth and branching of the evolutionary tree. Evolutionary Ecology 12:35–57. https://doi.org/10.1023/A:1006554906681.

Goss-Custard, J. D., S. E. A. Le V. Dit Durell, S. McGrorty, and C. J. Reading. 1982. Use of mussel *Mytilus edulis* beds by oystercatchers *Haematopus ostralegus* according to age and population size. Journal of Animal Ecology 51:543–554. https://doi.org/10.2307/3983.

Grimm, N. B., M. D. Staudinger, A. Staudt, S. L. Carter, F. S. Chapin, P. Kareiva, M. Ruckelshaus, and B. A. Stein. 2013. Climate-change impacts on ecological systems: introduction to a US assessment. Frontiers in Ecology and the Environment 11:456–464. https://doi.org/10.1890/120310.

Guill, C. 2009. Alternative dynamical states in stage-structured consumer populations. Theoretical Population Biology 76:168–178. https://doi.org/10.1016/j.tpb.2009.06.002.

Heberling, J. M., C. McDonough MacKenzie, J. D. Fridley, S. Kalisz, and R. B. Primack. 2019. Phenological mismatch with trees reduces wildflower carbon budgets. Ecology Letters 22:612–623. https://doi.org/10.1111/ele.13224.

Henson, S. A., H. S. Cole, J. Hopkins, A. P. Martin, and A. Yool. 2018. Detection of climate change-driven trends in phytoplankton phenology. Global Change Biology 24:e101–e111. https://doi.org/10.1111/gcb.13886.

Hjelm, J., and L. Persson. 2001. Size-dependent attack rate and handling capacity: inter-cohort competition in a zooplanktivorous fish. Oikos 95:520–532. https://doi.org/10.1034/j.1600-0706.2001.950317.x.

Hoegh-Guldberg, O., and J. F. Bruno. 2010. The impact of climate change on the world's marine ecosystems. Science 328:1523–1528. https://doi.org/10.1126/science.1189930.

Iwasa, Y., and S. A. Levin. 1995. The timing of life history events. Journal of Theoretical Biology 172:33–42. https://doi.org/10.1006/jtbi.1995.0003.

Iwasa, I., A. Pomiankowski, and S. Nee. 1991. The evolution of costly mate preferences. II. The "handicap" principle. Evolution 45:1431–1442. https://doi.org/10.1111/j.1558-5646.1991.tb02646.x.

Johansson, J., K. Bolmgren, and N. Jonzén. 2013. Climate change and the optimal flowering time of annual plants in seasonal environments. Global Change Biology 19:197–207. https://doi.org/10.1111/gcb.12006.

Jönsson, K. I., G. Herczeg, R. B. O'Hara, F. Söderman, A. F. Ter Schure, P. Larsson, and J. Merilä. 2009. Sexual patterns of prebreeding energy reserves in the common frog *Rana temporaria* along a latitudinal gradient. Ecography 32:831–839. https://doi.org/10.1111/j.1600-0587.2009.05352.x.

Jonzén, N., A. Hedenström, and P. Lundberg. 2007. Climate change and the optimal arrival of migratory birds. Proceedings of the Royal Society B 274:269–274. https://doi.org/10.1098/rspb.2006.3719.

King, D., and J. Roughgarden. 1982. Graded allocation between vegetative and reproductive growth for annual plants in growing seasons of random length. Theoretical Population Biology 22:1–16. https://doi.org/10.1016/0040-5809(82)90032-6.

Kjesbu, O. S., D. Righton, M. Krüger-Johnsen, A. Thorsen, K. Michalsen, M. Fonn, and P. R. Witthames 2010. Thermal dynamics of ovarian maturation in Atlantic cod (*Gadus morhua*). Canadian Journal of Fisheries and Aquatic Sciences 67:605–625. https://doi.org/10.1139/F10-011.

Knudsen, E., A. Lindén, C. Both, N. Jonzén, F. Pulido, N. Saino, W. J. Sutherland, et al. 2011. Challenging claims in the study of migratory birds and climate change. Biological Reviews 86:928–946. https://doi.org/10.1111/j.1469-185X.2011.00179.x.

Kooi, B., and T. Troost. 2006. Advantage of storage in a fluctuating environment. Theoretical Population Biology 70:527–541. https://doi.org/10.1016/j.tpb.2006.07.005.

Kooijman, S. A. L. M. 2000. Dynamic energy and mass budgets in biological systems. 2nd ed. Cambridge University Press, Cambridge.

Kristensen, N. P., J. Johansson, J. Ripa, and N. Jonzén. 2015. Phenology of two inter-dependent traits in migratory birds in response to climate change. Proceedings of the Royal Society B 282:20150288. https://doi.org/10.1098/rspb.2015.0288.

Lamb, E. G., and J. F. Cahill. 2006. Consequences of differing competitive abilities between juvenile and adult plants. Oikos 112:502–512. https://doi.org/10.1111/j.0030-1299.2006.14351.x.

Lamires, T. K., H. P. van der Jeugd, G. Eichhorn, A. M. Dokter, W. Bouten, M. P. Boom, K. E. Litvin, B. J. Ens, and B. A. Nolet. 2018. Arctic geese tune migration to a warming climate but still suffer from a phenological mismatch. Current Biology 28:2467–2473.e4. https://doi.org/10.1016/j.cub.2018.05.077.

Lande, R. 1979. Quantitative genetic analysis of multivariate evolution applied to brain:body size allometry. Evolution 33:402–416.

———. 1982. A quantitative genetic theory of life history evolution. Ecology 63:607–615.

Lindh, M., J. Johansson, K. Bolmgren, N. L. P. Lundström, Å. Brännström, and N. Jonzén. 2016. Constrained growth flips the direction of optimal phenological responses among annual plants. New Phytologist 209:1591–1599. https://doi.org/10.1111/nph.13706.

Lustenhouwer, N., R. A. Wilschut, J. L. Williams, W. H. van der Putten, and J. M. Levine. 2018. Rapid evolution of phenology during range expansion with recent climate change. Global Change Biology 24:e534–e544. https://doi.org/10.1111/gcb.13947.

McBride, R. S., S. Somarakis, G. R. Fitzhugh, A. Albert, N. A. Yaragina, M. J. Wuenshel, A. Alonso-Fernández, and G. Basilone. 2015. Energy acquisition and allocation to egg production in relation to fish reproductive strategies. Fish and Fisheries 16:23–57. https://doi.org/10.1111/faf.12043.

Meijer, T., and R. Drent. 1999. Re-examination of the capital and income dichotomy in breeding birds. Ibis 141:399–414. https://doi.org/10.1111/j.1474-919X.1999.tb04409.x.

Merilä, J., and A. P. Hendry. 2014. Climate change, adaptation, and phenotypic plasticity: the problem and the evidence. Evolutionary Applications 7:1–14. https://doi.org/10.1111/eva.12137.

Metz, J. A. J., and C. G. F. de Kovel. 2013. The canonical equation of adaptive dynamics for Mendelian diploids and haplo-diploids. Interface Focus 3:20130025. https://doi.org/10.1098/rsfs.2013.0025

Metz, J. A. J., S. A. H. Geritz, G. Meszéna, F. J. A. Jacobs, and J. S. van Heerwaarden. 1996. Adaptive dynamics: a geometrical study of the consequences of nearly faithful reproduction. Pages 183–231 *in* S. J. van Strien and S. M. Verduyn Lunel, eds. Stochastic and spatial structures of dynamical systems. North-Holland, Amsterdam.

Nicotra, A. B., O. K. Atkin, S. P. Bonser, A. M. Davidson, E. J. Finnegan, U. Mathesius, P. Poot, et al. 2010. Plant phenotypic plasticity in a changing climate. Trends in Plant Science 15:684–692. https://doi.org/10.1016/j.tplants.2010.09.008.

Norris, D. R., P. Marra, R. Montgomerie, T. Kyser, and L. Ratcliffe. 2004. Reproductive effort, molting latitude, and feather color in a migratory songbird. Science 306:2249–2250. https://doi.org/10.1126/science.1103542.

Nussey, D. H., A. J. Wilson, and J. E. Brommer. 2007. The evolutionary ecology of individual phenotypic plasticity in wild populations. Journal of Evolutionary Biology 20:831–844. https://doi.org/10.1111/j.1420-9101.2007.01300.x.

Parmesan, C., N. Ryrholm, C. Stefanescu, J. K. Hill, C. D. Thomas, H. Descimon, B. Huntley, et al. 1999. Poleward shifts in geographical ranges of butterfly species associated with regional warming. Nature 399:579–583. https://doi.org/10.1038/21181.

Persson, L. 1985. Asymmetrical competition: are larger animals competitively superior? American Naturalist 126:261–266. https://doi.org/10.1086/284413.

Persson, L., and A. M. de Roos. 2013. Symmetry breaking in ecological systems through different energy efficiencies of juveniles and adults. Ecology 94:1487–1498. https://doi.org/10.1890/12-1883.1.

Persson, L., K. Leonardsson, A. M. de Roos, M. Gyllenberg, and B. Christensen. 1998. Ontogenetic scaling of foraging rates and the dynamics of a size-structured consumer-resource model. Theoretical Population Biology 54:270–293. https://doi.org/10.1006/tpbi.1998.1380.

Piao, S., Q. Liu, A. Chen, I. A. Janssens, Y. Fu, J. Dai, L. Liu, X. Lian, M. Shen, and X. Zhu. 2019. Plant phenology and global climate change: current progresses and challenges. Global Change Biology 25:1922–1940. https://doi.org/10.1111/gcb.14619.

Réale, D., A. G. McAdam, S. Boutin, and D. Berteaux. 2003. Genetic and plastic responses of a northern mammal to climate change. Proceedings of the Royal Society B 270:591–596. https://doi.org/10.10.1098/rspb.2002.2224.

Renner, S. S., and C. M. Zohner. 2018. Climate change and phenological mismatch in trophic interactions among plants, insects, and vertebrates. Annual Review of Ecology, Evolution, and Systematics 49:165–182. https://doi.org/10.1146/annurev-ecolsys-110617-062535.

Richardson, A. J., and D. S. Schoeman. 2004. Climate impact on plankton ecosystems in the Northeast Atlantic. Science 305:1609–1612. https://doi.org/10.1126/science.1100958.

Roff, D. A. 1992. The evolution of life histories. Chapman & Hall, London.

Roy, D. B., and T. H. Sparks. 2000. Phenology of British butterflies and climate change. Global Change Biology 6:407–416. https://doi.org/10.1046/j.1365-2486.2000.00322.x.

Sainmont, J., K. H. Anderson, Ø. Varpe, and A. W. Visser. 2014. Capital versus income breeding in a seasonal environment. American Naturalist 184:466–476. https://doi.org/10.1086/677926.

Schoener, T. W. 1983. Field experiments on interspecific competition. American Naturalist 122:240–285. https://doi.org/10.1086/284133.

Sénéchal, É., J. Bêty, H. G. Gilchrist, K. A. Hobson, and S. E. Jamieson. 2011. Do purely capital layers exist among flying birds? evidence of exogenous contribution to arctic-nesting common eider eggs. Oecologia 165:593–604. https://doi.org/10.1007/s00442-010-1853-4.

Sol, D., D. M. Santos, J. Garcia, and M. Cuadrado. 1998. Competition for food in urban pigeons: the cost of being juvenile. Condor 100:298–304. https://doi.org/10.2307/1370270.

Stearns, S. C. 1992. The evolution of life histories. Oxford University Press, London.

Stenseth, N. C., and A. Mysterud. 2002. Climate, changing phenology, and other life history traits: nonlinearity and match–mismatch to the environment. Proceedings of the National Academy of Sciences of the USA 99:13379–13381. https://doi.org/10.1073/pnas.212519399.

Stephens, P. A., I. L. Boyd, J. M. McNamara, and A. I. Houston. 2009. Capital breeding and income breeding: their meaning, measurement, and worth. Ecology 90:2057–2067. https://doi.org/10.1890/08-1369.1.

Sun, Z., and A. M. de Roos. 2017. Seasonal reproduction leads to population collapse and an Allee effect in a stage-structured consumer-resource model when mortality rate increases. PLoS One 12:e0187338. https://doi.org/10.1371/journal.pone.0187338.

Sutherland, W. J. 1996. From individual behaviour to population ecology. Oxford University Press, Oxford.

Thackeray, S. J., P. A. Henrys, D. Hemming, J. R. Bell, M. S. Botham, S. Burthe, and S. Wanless. 2016. Phenological sensitivity to climate across taxa and trophic levels. Nature 535:241–245. https://doi.org/10.1038/nature18608.

van Asch, M., L. Salis, L. J. M. Holleman, B. van Lith, and M. E. Visser. 2013. Evolutionary response of egg hatching date of a herbivorous insect under climate change. Nature Climate Change 3:244–248. https://doi.org/10.1038/nclimate1717.

Vimercati, G., S. J. Davies, and J. Measey. 2019. Invasive toads adopt marked capital breeding when introduced to a cooler, more seasonal environment. Biological Journal of the Linnean Society 128:657–671. https://doi.org/10.1093/biolinnean/blz119.

Visser, M. E., A. J. van Noordwijk, J. M. Tinbergen, and C. M. Lessells. 1998. Warmer springs lead to mistimed reproduction in great tits (*Parus major*). Proceedings of the Royal Society B 265:1867–1870. https://doi.org/10.1098/rspb.1998.0514.

Williams, C. T., J. E. Lane, M. M. Humphries, A. G. McAdam, and S. Boutin. 2014. Reproductive phenology of a food-hoarding mast-seed consumer: resource- and density-dependent benefits of early breeding in red squirrels. Oecologia 174:777–788. https://doi.org/10.1007/s00442-013-2826-1.

Yamamura, N., N. Fujita, M. Hayashi, Y. Nakamura, and A. Yamauchi. 2007. Optimal phenology of annual plants under grazing pressure. Journal of Theoretical Biology 246:530–537. https://doi.org/10.1016/j.jtbi.2007.01.010.

Associate Editor: Sébastien Lion
Editor: Russell Bonduriansky

"His courage and perseverance were, however, equal to the situation, and he resolutely declined to return home in the autumn. A fourth winter found him still in his igloo at his old quarters." Figured: "Aurora sketched by Hall." From "Hall's Second Arctic Expedition" by Ellis Hornor Yarnall (*The American Naturalist*, 1880, 14:332–347).